

Two-Loop QCD Corrections to the Higgs plus three-parton amplitudes with Top Mass Correction

Qingjun Jin^{a,b} and Gang Yang^{a,c}

^a*CAS Key Laboratory of Theoretical Physics, Institute of Theoretical Physics, Chinese Academy of Sciences, Beijing 100190, China*

^b*Graduate School of China Academy of Engineering Physics, No. 10 Xibeiwang East Road, Haidian District, Beijing, 100193, China*

^c*School of Physical Sciences, University of Chinese Academy of Sciences, No. 19A Yuquan Road, Beijing 100049, China*

E-mail: qjin@gscaep.ac.cn, yangg@itp.ac.cn

ABSTRACT: We obtain the two-loop QCD corrections to Higgs plus three-parton amplitudes with dimension-seven operators in Higgs effective field theory. This provides the two-loop S-matrix elements for Higgs plus one-jet production at LHC with top-mass correction. We apply efficient unitarity plus IBP methods which are described in detail. We also study the color decomposition of the fermion cuts and find a connection between fundamental and adjoint representations which can reduce non-planar to planar unitarity cuts. We obtain final results in simple analytic form which exhibits intriguing hidden structure. The principle of maximal transcendentality is found to be satisfied for all results. The lower transcendentality parts also contain universal building blocks and can be written in compact analytic forms, suggesting further hidden structures.

Contents

1	Introduction	2
2	Preparations	4
2.1	Operator basis	4
2.2	Divergence structure	5
3	Computation with unitarity-IBP	7
3.1	D -dimensional unitary cut	8
3.2	Gauge invariant basis	9
3.3	Planar unitarity cut	11
4	Color decomposition of fermion cuts	14
4.1	Color decomposition of tree amplitudes	14
4.2	The s_{12} two double-cut	15
4.3	The s_{12} triple-cut	17
4.4	Other cuts	17
5	Results	18
5.1	Tree-level results	19
5.2	Loop corrections	19
5.3	Operator mixing	22
6	Discussion	23
A	One-loop results	25
B	Two-loop remainder of $F_{\hat{\mathcal{O}}_1}$	25
B.1	$\hat{\mathcal{O}}_1 \rightarrow (1^-, 2^-, 3^-)$	26
B.2	$\hat{\mathcal{O}}_1 \rightarrow (1^-, 2^-, 3^+)$	27
B.3	$\hat{\mathcal{O}}_1 \rightarrow (1^q, 2^{\bar{q}}, 3^-)$	27
C	Two-loop remainder of $F_{\hat{\mathcal{O}}_3}$	27
D	Two-loop remainder of $F_{\hat{\mathcal{O}}_4}$	28
D.1	$\hat{\mathcal{O}}_4 \rightarrow (1^-, 2^-, 3^-)$	28
D.2	$\hat{\mathcal{O}}_4 \rightarrow (1^-, 2^-, 3^+)$	28
D.3	$\hat{\mathcal{O}}_4 \rightarrow (1^q, 2^{\bar{q}}, 3^-)$	30

1 Introduction

Scattering amplitude plays an indispensable role in particle physics. It acts as a bridge between a theoretical model and the experimental data. The Large Hadron Collider (LHC) verified the correctness of the standard model and discovered the last particle of the standard model of particle physics, the Higgs particle [1, 2]. The proposed future colliders, such as the circular electron-positron collider (CEPC) in China [3, 4] and the future circular collider (FCC) at CERN [5–7], will have more accuracy and less background noise. One main object of the present and future collider experiments is to understand more precisely the Higgs properties and the mechanism of electroweak symmetry breaking. It is also possible to find signs beyond the standard model, such as supersymmetry, dark matter, etc. In order to compare with the experimental data, we need to calculate the scattering amplitude to the next-to-next-to leading order (NNLO) or even higher orders. This is usually beyond the capabilities of traditional Feynman diagram methods. Fortunately, during last thirty years, in the field of amplitude calculation, many new methods and tools have been developed, including the spinor helicity formalism [8–11], the unitarity cut method [12–14], and recursion relations [15–17]. These methods have achieved great success in the calculation of the scattering amplitude, not only in supersymmetric field theories, but also in realistic QCD.

In this paper, we study the Higgs plus three-parton amplitudes in standard model. Our motivation is twofold. First, the precise theoretical prediction of Higgs scattering process is highly demanded to match the improving experiment precision. At LHC, the dominant Higgs production channel is the gluon fusion through a top quark loop [18, 19]. The computation of this process can be simplified using an effective field theory (EFT) in which the top quark is integrated out [20–26]. This EFT is valid in the approximation that the top mass m_t is much larger than Higgs mass m_H . The leading term in the effective Lagrangian is a unique dimension-5 operator, $H\text{tr}(F_{\mu\nu}F^{\mu\nu})$, where H is the Higgs field and $F_{\mu\nu}$ is the gauge field strength. The two-loop QCD corrections to Higgs plus three-parton amplitudes with leading dimension-5 operator were computed in [27], which has been used in computing the cross sections of Higgs plus a jet production at N²LO [28–34] in the infinite top mass limit. When the Higgs transverse momentum is comparable to the top mass, the contribution of higher dimension operators in the Higgs EFT will be important. This has been taken into account so far only at NLO QCD accuracy, including the finite top mass effect [35–37]. A concrete goal of this paper is to compute the two-loop QCD corrections for Higgs plus 3-parton amplitudes with dimension-7 operators in the Higgs EFT. This provides, for the first time at N²LO QCD accuracy, the S-matrix elements of the top mass correction for Higgs plus a jet production.

Another motivation for our calculation is to study analytic properties of amplitudes. Analytic study is crucial for uncovering hidden structures of the amplitudes. One particular focus of the paper is related to the so-called maximal transcendentality principle (MTP). Transcendentality is a mathematical quantity used to characterize the algebraic complexity of a function. The principle of maximal transcendentality conjectures that the algebraically most complex part of certain physical observables in QCD and $\mathcal{N} = 4$ SYM are equal.

This was first proposed in [38, 39] that, the anomalous dimensions of twist-two operators in $\mathcal{N} = 4$ SYM can be obtained from the maximally transcendental part of the QCD results [40]. In these quantities, the transcendentality degree is governed by the multi-zeta values. Intriguingly, the principle can be extended to the Higgs and three-parton amplitudes or form factors, which involves complicated two dimensional Harmonic Polylogarithms [41, 42]. This was first observed for the $\text{Tr}(F^2) \rightarrow 3g$ form factors [43], which on one side corresponds to the QCD correction to the Higgs to 3 parton amplitudes in the large top quark mass limit [27], and on the other side is equivalent to the form factor of stress-tensor multiplet in $\mathcal{N} = 4$ SYM. The universal structure of the maximal transcendentality were also found in form factors of more general operators in $\mathcal{N} = 4$ SYM [44–48]. The principle was also verified for other quantities like Wilson lines [49, 50]. It has also been also applied to compute collinear anomalous dimensions [51]. Recently, the MTP was also verified for three gluon form factors of the the dimension-6 operators in the pure gluon sector [52–55]. In this paper, as also reported in [56], the principle was extended to the two-quark one-gluon form factors. With a simple replacement of the $SU(N)$ quadratic Casimir $C_F \rightarrow C_A$, the maximally transcendental (MT) part of $H \rightarrow q\bar{q}g$ form factors were found to reduce to the MT part of $H \rightarrow 3g$ form factors.

Furthermore, as we will see, not only the maximally transcendental part, the parts of lower transcendentality degrees also exhibit certain universality. The degree-3 parts can be constructed by a building block T_3 , plus simple log functions and constants. The degree-2 parts also contain a building block T_2 . Using these building blocks, the amplitudes can be written in compact forms. These suggest the hidden structure and simplicity also exist for lower transcendental parts. Exploring them further will be very important for computing the full QCD results.

Our computations employ a new strategy of combining unitarity cut [12–14] and integration by parts (IBP) method [57, 58]. IBP reduces the loop integrands to a small set of master integrals. Instead of applying IBP to the full loop amplitude, we apply cut IBP to the cut integrand. Our new strategy increased the efficiency of IBP by an order of magnitude. Similar ideas of combining unitarity cut and IBP reduction has also been used in [59], see also [60–65]. The pure gluon sector of two-loop $H \rightarrow 3g$ amplitudes contain only the leading color contribution, in which the loop integrands can be conveniently obtained using the planar unitarity method. In the presence of internal quarks, more complicated color structures appears. We will show that by making connection between fermions in fundamental and adjoint representations, a color decomposition is possible such that the full two-loop integrand can be constructed using planar cuts.

This paper is organized as follows. In Sect. 2, we introduce the operators in Higgs EFT and describe the divergences structure. In Sect. 3, we describe the details of the computation using cut-IBP strategy. In Sect. 4, we discuss the color decomposition of amplitudes that involve internal quarks. In Sect. 5, we present the analytic expressions of form factors. We conclude and discuss the transcendentality properties in Sect. 6. Appendix A–D provides expression of one-loop and two-loop results.

2 Preparations

2.1 Operator basis

Higgs can be produced from the gluon fusion through a heavy quark loop at LHC. The Yukawa couplings between Higgs and quarks are proportional to the mass of quarks, so the diagrams with a top quark loop dominate. Integrating out the top quark renders the Higgs effective field theory (HEFT) [20–26]:

$$\mathcal{L}_{\text{eff}} = \hat{C}_0 H \mathcal{O}_0 + \frac{1}{m_t^2} \sum_{i=1}^4 \hat{C}_i H \mathcal{O}_i + \mathcal{O}\left(\frac{1}{m_t^4}\right), \quad (2.1)$$

where H is the Higgs field, $\mathcal{O}_0 = \text{tr}(F^2)$ is the leading term, and the subleading terms contain dimension-6 operators [66–70]

$$\mathcal{O}_1 = \text{tr}(F_\mu^\nu F_\nu^\rho F_\rho^\mu), \quad (2.2)$$

$$\mathcal{O}_2 = \text{tr}(D_\rho F_{\mu\nu} D^\rho F^{\mu\nu}), \quad (2.3)$$

$$\mathcal{O}_3 = \text{tr}(D^\rho F_{\rho\mu} D_\sigma F^{\sigma\mu}), \quad (2.4)$$

$$\mathcal{O}_4 = \text{tr}(F_{\mu\rho} D^\rho D_\sigma F^{\sigma\mu}). \quad (2.5)$$

The last two operators have zero contribution in the pure gluon sector and only contribute when there are internal light quark lines. In this paper we consider the results including complete massless quarks contributions.

An amplitude with a Higgs boson and n gluons is equivalent to the form factor with an operator \mathcal{O}_i in the EFT (2.1):

$$\mathcal{F}_{\mathcal{O}_i, n} = \int d^4x e^{-iq \cdot x} \langle p_1, \dots, p_n | \mathcal{O}_i(x) | 0 \rangle. \quad (2.6)$$

where $q^2 = m_H^2$. In the following, we will often refer Higgs amplitudes as form factors.

Using Bianchi identity one can decompose the operator \mathcal{O}_2 as (see e.g. [67])

$$\mathcal{O}_2 = \frac{1}{2} \partial^2 \mathcal{O}_0 - 4 g_{\text{YM}} \mathcal{O}_1 + 2 \mathcal{O}_4. \quad (2.7)$$

The relation can be transformed into a relation of the form factors,

$$\mathcal{F}_{\mathcal{O}_2} = \frac{1}{2} q^2 \mathcal{F}_{\mathcal{O}_0} - 4 g_{\text{YM}} \mathcal{F}_{\mathcal{O}_1} + 2 \mathcal{F}_{\mathcal{O}_4}, \quad (2.8)$$

where the partial derivatives reduce to square of q which is the total momentum flowing through the \mathcal{O}_0 operator. This relation will serve as a self-consistency check for our computation.

We can classify the operators according to their *length*. Naturally, the length of an operator \mathcal{O} is the number of elementary fields (A , $\bar{\psi}$ and ψ) in its lowest expansion (i.e. with minimal number of elementary fields). For example $\text{tr}(F^2) \sim \text{tr}(\partial^2 A^2)$ has length 2, and

$\text{tr}(F^3) \sim \text{tr}(\partial^3 A^3)$ has length 3. A form factor of an operator is called “minimal” if the form factor contains exactly the same number of on shell particles as that of the lowest expansion of the operator. For example $\text{tr}(F^3) \rightarrow ggg$ and $\epsilon_{ijk}\psi^i\psi^j\psi^k \rightarrow qq\bar{q}$ are minimal form factors, but $\text{tr}(F^2) \rightarrow g\bar{q}q$ is a non-minimal form factor.

Sometimes this “naive” definition results in a zero minimal tree form factor. As an example, for \mathcal{O}_4 the 2 gluon form factor vanishes, and the simplest non-zero form factor is $\mathcal{O}_4 \rightarrow q\bar{q}g$. The reason is that, using the equation of motion $D_\sigma F^{\sigma\mu} \sim g \sum_i (\bar{\psi}_i \gamma^\nu T^a \psi_i)$, \mathcal{O}_4 is equivalent to $\mathcal{O}'_4 = F_{\mu\nu}^a D^\mu \sum_i (\bar{\psi}_i \gamma^\nu T^a \psi_i)$, which is a length-3 operator. The more proper definition is that, the minimal form factor for a given operator is the simplest form factor which is non-zero at tree level, and the length of the operator is the number of external on-shell states in the minimal form factor. Using this definition, \mathcal{O}_4 has length 3, and its minimal form factor is $\mathcal{O}_4 \rightarrow q\bar{q}g$. \mathcal{O}_3 has length 4, and its minimal form factor is $\mathcal{O}_3 \rightarrow qq\bar{q}\bar{q}$.

2.2 Divergence structure

Form factors contain both UV and IR divergences. We apply dimensional regularization ($D = 4 - 2\epsilon$) in the conventional dimension regularization (CDR) scheme, and we use the modified minimal subtraction renormalization ($\overline{\text{MS}}$) scheme [71]. For IR divergences, we apply the Catani subtraction formula [72]. Below we describe these in detail.

To begin with, the bare form factor can be expanded as

$$\mathcal{F}_b = g_0^{\delta_n} \left[\mathcal{F}_b^{(0)} + \frac{\alpha_0}{4\pi} \mathcal{F}_b^{(1)} + \left(\frac{\alpha_0}{4\pi} \right)^2 \mathcal{F}_b^{(2)} + \mathcal{O}(\alpha_0^3) \right], \quad (2.9)$$

where $g_0 = g_{\text{YM}}$ is the bare gauge coupling and $\alpha_0 = \frac{g_0^2}{4\pi}$. We pull out the coupling $g_0^{\delta_n} = g_0^{n-\mathbb{L}}$ in the tree form factor, which depends on the number of external legs n and the length of the operator \mathbb{L} .

The renormalization of the UV divergences can be implemented in two steps, one for the coupling constant and one for the local operator.

First, we express the bare gauge coupling α_0 in terms of the renormalized coupling $\alpha_s = \alpha_s(\mu^2) = \frac{g_s(\mu^2)^2}{4\pi}$, evaluated at the renormalization scale μ^2 , as

$$\alpha_0 = \alpha_s S_\epsilon^{-1} \frac{\mu^{2\epsilon}}{\mu_0^{2\epsilon}} \left[1 - \frac{\beta_0}{\epsilon} \frac{\alpha_s}{4\pi} + \left(\frac{\beta_0^2}{\epsilon^2} - \frac{\beta_1}{2\epsilon} \right) \left(\frac{\alpha_s}{4\pi} \right)^2 + \mathcal{O}(\alpha_s^3) \right], \quad (2.10)$$

where $S_\epsilon = (4\pi e^{-\gamma_E})^\epsilon$ is due to the use of $\overline{\text{MS}}$ scheme, and μ_0^2 is the scale introduced to keep gauge coupling dimensionless in the bare Lagrangian. The first two coefficients of the β function are¹

$$\beta_0 = \frac{11C_A}{3} - \frac{2n_f}{3}, \quad \beta_1 = \frac{34C_A^2}{3} - \frac{10C_A n_f}{3} - 2C_F n_f, \quad (2.11)$$

¹Since in our result n_f is always associated with a factor t_F in $\text{Tr}(T^a T^b) = t_F \delta^{ab}$, we simply set $t_F = 1/2$.

where n_f is the flavor number of fermions and the quadratic Casimirs in the adjoint and fundamental representations are respectively

$$C_A = N_c, \quad C_F = \frac{N_c^2 - 1}{2N_c}. \quad (2.12)$$

Second, we renormalize the operator by introducing the renormalization constant Z for the operator

$$Z = 1 + \sum_{l=1}^{\infty} \left(\frac{\alpha_s}{4\pi} \right)^l Z^{(l)}. \quad (2.13)$$

The anomalous dimension can be computed from the renormalization constant as

$$\gamma = \mu \frac{\partial}{\partial \mu} \log Z = \sum_{l=1}^{\infty} \left(\frac{\alpha_s}{4\pi} \right)^l \gamma^{(l)}. \quad (2.14)$$

Using (2.13) and note that $\mu \frac{\partial}{\partial \mu} \alpha_s(\mu) = -2\epsilon \alpha_s - \frac{\beta_0}{2\pi} \alpha_s^2 + \mathcal{O}(\alpha_s^3)$, we have

$$\gamma^{(1)} = 2\epsilon Z^{(1)}, \quad (2.15)$$

$$\gamma^{(2)} = 4\epsilon Z^{(2)} - 2\epsilon (Z^{(1)})^2 + 2Z^{(1)} \beta_0. \quad (2.16)$$

Since γ is finite, it is clear that the $\frac{1}{\epsilon^2}$ part in $Z^{(2)}$ is fixed by one-loop results as

$$Z^{(2)} \Big|_{\frac{1}{\epsilon^2}\text{-part.}} = \frac{1}{2} (Z^{(1)})^2 - \frac{1}{2\epsilon} Z^{(1)} \beta_0. \quad (2.17)$$

Expanding the renormalized form factor as

$$\mathcal{F} \equiv Z \mathcal{F}_b = g_s^{\delta_n} S_\epsilon^{-\delta_n/2} \sum_{l=0}^{\infty} \left(\frac{\alpha_s}{4\pi} \right)^l \mathcal{F}^{(l)}, \quad (2.18)$$

we have the relations between the renormalized components $\mathcal{F}^{(l)}$ and the bare ones $\mathcal{F}_b^{(l)}$ as

$$\mathcal{F}^{(0)} = \mathcal{F}_b^{(0)}, \quad (2.19)$$

$$\mathcal{F}^{(1)} = S_\epsilon^{-1} \mathcal{F}_b^{(1)} + \left(Z^{(1)} - \frac{\delta_n \beta_0}{2\epsilon} \right) \mathcal{F}_b^{(0)}, \quad (2.20)$$

$$\begin{aligned} \mathcal{F}^{(2)} &= S_\epsilon^{-2} \mathcal{F}_b^{(2)} + S_\epsilon^{-1} \left[Z^{(1)} - \left(1 + \frac{\delta_n}{2} \right) \frac{\beta_0}{\epsilon} \right] \mathcal{F}_b^{(1)} \\ &+ \left[Z^{(2)} - \frac{\delta_n \beta_0}{2\epsilon} Z^{(1)} + \frac{\delta_n^2 + 2\delta_n \beta_0^2}{8\epsilon^2} - \frac{\delta_n \beta_1}{4\epsilon} \right] \mathcal{F}_b^{(0)}. \end{aligned} \quad (2.21)$$

The renormalized form factor contains only IR divergences, which take a universal structure [72, 73] (see also [27]):

$$\mathcal{F}^{(1)} = I^{(1)}(\epsilon) \mathcal{F}^{(0)} + \mathcal{F}^{(1),\text{fin}} + \mathcal{O}(\epsilon), \quad (2.22)$$

$$\mathcal{F}^{(2)} = I^{(2)}(\epsilon) \mathcal{F}^{(0)} + I^{(1)}(\epsilon) \mathcal{F}^{(1)} + \mathcal{F}^{(2),\text{fin}} + \mathcal{O}(\epsilon), \quad (2.23)$$

where for the form factor with n external gluons, we have

$$I_{ng}^{(1)}(\epsilon) = -\frac{e^{\gamma_E \epsilon}}{\Gamma(1-\epsilon)} \left(\frac{C_A}{\epsilon^2} + \frac{\beta_0}{2\epsilon} \right) \sum_{i=1}^n (-s_{i,i+1})^{-\epsilon}, \quad (2.24)$$

$$I_{ng}^{(2)}(\epsilon) = -\frac{1}{2} [I^{(1)}(\epsilon)]^2 - \frac{\beta_0}{\epsilon} I^{(1)}(\epsilon) + \frac{e^{-\gamma_E \epsilon} \Gamma(1-2\epsilon)}{\Gamma(1-\epsilon)} \left[\frac{\beta_0}{\epsilon} + \mathcal{K} \right] I^{(1)}(2\epsilon) + n \frac{e^{\gamma_E \epsilon}}{\epsilon \Gamma(1-\epsilon)} \mathcal{H}_{\Omega,g}^{(2)}.$$

For the case with external quarks, we have

$$I_{q\bar{q}g}^{(1)}(\epsilon) = -\frac{e^{\gamma_E \epsilon}}{\Gamma(1-\epsilon)} \left[\left(\frac{C_A}{\epsilon^2} + \frac{3C_A}{4\epsilon} + \frac{\beta_0}{4\epsilon} \right) ((-s_{13})^{-\epsilon} + (-s_{23})^{-\epsilon}) - \frac{1}{C_A} \left(\frac{1}{\epsilon^2} + \frac{3}{2\epsilon} \right) (-s_{12})^{-\epsilon} \right], \quad (2.25)$$

$$I_{q\bar{q}g}^{(2)}(\epsilon) = -\frac{1}{2} [I^{(1)}(\epsilon)]^2 - \frac{\beta_0}{\epsilon} I^{(1)}(\epsilon) + \frac{e^{-\gamma_E \epsilon} \Gamma(1-2\epsilon)}{\Gamma(1-\epsilon)} \left[\frac{\beta_0}{\epsilon} + \mathcal{K} \right] I^{(1)}(2\epsilon) + \frac{e^{\gamma_E \epsilon}}{\epsilon \Gamma(1-\epsilon)} \mathcal{H}_{\Omega}^{(2)},$$

where

$$\mathcal{K} = \left(\frac{67}{9} - \frac{\pi^2}{3} \right) C_A - \frac{10}{9} n_f, \quad (2.26)$$

and

$$\mathcal{H}_{\Omega}^{(2)} = 2\mathcal{H}_{\Omega,q}^{(2)} + \mathcal{H}_{\Omega,g}^{(2)}, \quad (2.27)$$

$$\mathcal{H}_{\Omega,g}^{(2)} = \left(\frac{\zeta_3}{2} + \frac{5}{12} + \frac{11\pi^2}{144} \right) C_A^2 + \frac{5n_f^2}{27} - \left(\frac{\pi^2}{72} + \frac{89}{108} \right) C_A n_f - \frac{n_f}{4C_A}, \quad (2.28)$$

$$\begin{aligned} \mathcal{H}_{\Omega,q}^{(2)} &= \left(\frac{7\zeta_3}{4} + \frac{409}{864} - \frac{11\pi^2}{96} \right) C_A^2 - \left(\frac{\zeta_3}{4} + \frac{41}{108} + \frac{\pi^2}{96} \right) - \left(\frac{3\zeta_3}{2} + \frac{3}{32} - \frac{\pi^2}{8} \right) \frac{1}{C_A} \\ &+ \left(\frac{\pi^2}{48} - \frac{25}{216} \right) 2C_F n_f. \end{aligned} \quad (2.29)$$

3 Computation with unitarity-IBP

The traditional method of computing scattering amplitudes is based on Feynman diagrams. In multiloop calculations, the efficiency of the Feynman diagram is relatively low. Because when the scattering amplitude is split into many Feynman diagrams, the gauge symmetry, unitarity and other properties of the scattering amplitude are destroyed. The unitarity-cut method uses tree amplitudes as building blocks to construct the integrand of loop amplitudes [12–14]. In this construction, the original properties and symmetry of the amplitude are preserved, so that the integrand can be calculated much more efficiently. The integration by parts (IBP) method can be used to reduce the integrals further to a small set of master integrals [57, 58].

The commonly used strategy of unitarity method is to reconstruct the full integrand using a set of unitarity cuts. The complete integrand can be written as the sum of a set of integrals, together with some coefficients which are polynomials of spacetime dimension D and are rational in the momentum invariants. Each unitarity cut fixes some coefficients, and

different unitarity cuts will be applied successively until all the coefficients are fixed. After the full integrand is obtained, it can be reduced using IBP. We illustrate the above procedure as:

$$\mathcal{F}^{(l)} \Big|_{\text{cut}} \xrightarrow{\text{reconstruction}} \mathcal{F}^{(l)} = \sum_a C_a I_a \xrightarrow{\text{IBP}} \sum_i c_i M_i, \quad (3.1)$$

where M_i are IBP master integrals.

This strategy has two drawbacks. First, rebuilding a complete integrand is not a trivial task. The labelings of loop momenta in different unitarity cuts are usually different from each other. So the reconstruction of the full integrand involves cumbersome shifting and redefinition of loop momenta, especially when non-planar graphs are involved.² Second, the IBP reduction of the full integrand can be very slow. IBP usually takes a long time and consume a lot of computing resources, and it is sometimes the main bottleneck in the whole calculation.

We use a new strategy of combining IBP and unitarity cut which helps to overcome both issues. The key idea is that instead of applying IBP to the full loop amplitude, we apply IBP directly to each cut integrand:

$$\mathcal{F}^{(l)} \Big|_{\text{cut}} = \sum_a C_a I_a \Big|_{\text{cut}} \xrightarrow{\text{cut-IBP}} \sum_{\text{cut permitted}} c_i M_i \xrightarrow{\text{collect}} \sum_i c_i M_i. \quad (3.2)$$

If a master integral allows a given unitarity cut, this cut will be enough to determine the *final* coefficient of the master integral. A single unitarity cut only fixes the coefficients of a subset of master integrals. We apply different unitarity cuts successively, until all the coefficients are fixed. In this way, there is no need to construct the full integrand, but one reaches directly to the finally coefficients c_i of IBP master integrals. Furthermore, during IBP, imposing the cut condition drops a lot of integrals and makes a lot of sectors trivial. IBP with cut condition is much faster than the complete IBP. Our strategy increased the efficiency of IBP by an order of magnitude. A further important bonus of the cut-IBP method is that different cuts can provide internal consistency checks, which are very helpful in complicated cases. Later we will explain our strategy in more details.

3.1 D -dimensional unitary cut

Four-dimensional spinor helicity formalism is very powerful in the computation of supersymmetric gauge theory amplitudes. However, in the computation of non-supersymmetric theory amplitudes, it fails to capture the rational terms (see e.g. [74–76]). We will apply the planar D -dimensional unitarity method in the computation of $H \rightarrow 3g$ amplitude. In the pure gluon sector the non-planar contribution vanishes at 2 loops [53] and the amplitude is proportional to the simple color factor N_c^2 , so the planar unitarity cut gives the full result. In the presence of internal quark legs, the amplitude contain N_c^0 and N_c^{-2} contributions. However, as will be shown in Sect. 4, we can still use planar cuts, if we assign proper color factors to different

²This problem can be avoided in planar graphs by using zone variables.

internal-state configurations. So these contributions are not intrinsically non-planar. The planar unitarity cut is not suffice in the computation of $H \rightarrow q\bar{q}g$ amplitude, which contains some intrinsic non-planar contributions. We compute them using Feynman diagrams with FeynArts [77]. One may also carry out the non-planar unitarity cut, in which the building blocks will be the complete amplitudes (form factors) with color factors.

Tree amplitudes and form factors can be computed using planar Feynman diagrams, or recursion relations [15–17]. The polarization vectors of cut internal gluons satisfy the following contraction rule

$$\varepsilon^\mu(p) \circ \varepsilon^\nu(p) \equiv \sum_{\text{helicities}} \varepsilon^\mu(p)\varepsilon^\nu(p) = \eta^{\mu\nu} - \frac{q^\mu p^\nu + q^\nu p^\mu}{q \cdot p}, \quad (3.3)$$

where q^μ is an arbitrary reference momenta. The q -dependent terms vanish due to gauge invariance, and disappear in the full cut-amplitude. The quark (or anti-quark) field also has two external states, denoted by $u_s(p)$ (or $\bar{u}_s(p)$), which are the solutions of the (massless) Dirac equation. For sum of quark states, one uses

$$u_s(p) \circ \bar{u}_s(p) \equiv \sum_s u_s(p)\bar{u}_s(p) = \not{p}. \quad (3.4)$$

Comparing with the 4-dimensional unitarity cut in spinor helicity formalism, the D -dimensional unitarity method usually generates much larger expressions in the intermediate steps. As a compensation, the D -dimensional unitarity method not only captures all rational-type terms, but also produces integrals with regular propagators, which is ready for IBP reduction. In contrast, in the case of 4-dimensional unitarity cut, a reconstruction must be performed to convert the spinor-brackets to standard propagators.

3.2 Gauge invariant basis

The cut-integrand is explicitly gauge invariant, since all its tree building blocks are gauge invariant. This means the cut-integrand vanishes if any $\varepsilon_i \rightarrow p_i$, even before IBP is performed. This explicit gauge invariance serves as a self-consistence check of our cut-integrand. By contrast, the complete *uncut*-loop integrand is typically not explicitly gauge invariant, setting $\varepsilon_i \rightarrow p_i$ leaves some scaleless integrals which are zero after integration.

Since amplitude is gauge invariant, we can expand it using a set of gauge invariant basis B_α (see e.g. [27] and also [59, 78] for recent general discussion):

$$\mathcal{F}_n(\varepsilon_i, p_i, l_a) = \sum_\alpha f_n^\alpha(p_i, l_a) B_\alpha. \quad (3.5)$$

The coefficients $f_n^\alpha(p_i, l_a)$ can be computed as

$$f_n^\alpha(p_i, l_a) = B^\alpha \circ \mathcal{F}_n(\varepsilon_i, p_i, l_a), \quad (3.6)$$

where the dual basis B^α play as projectors, which satisfies,

$$B^\alpha \circ B_\beta = \delta_\beta^\alpha, \quad B_\alpha = G_{\alpha\beta} B^\beta, \quad G_{\alpha\beta} = B_\alpha \circ B_\beta. \quad (3.7)$$

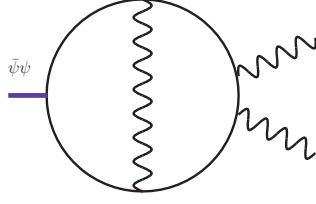


Figure 1. A fermion loop containing $\bar{\psi}\psi \in O_{\text{even}}$. The gamma trace contains 9 gamma matrices (5 from fermion propagators and 4 from quark-gluon vertices) and thus vanishes.

The ‘o’ product is defined in (3.3) and (3.4).

For the form factor with three gluons, the gauge invariant basis has 4 elements and we can choose the basis as

$$B_1 = A_1 C_{23}, \quad B_2 = A_2 C_{31}, \quad B_3 = A_3 C_{12}, \quad B_4 = A_1 A_2 A_3, \quad (3.8)$$

in which A_i and C_{ij} are defined by

$$A_i = \frac{\varepsilon_i \cdot p_j}{p_i \cdot p_j} - \frac{\varepsilon_i \cdot p_k}{p_i \cdot p_k}, \quad C_{ij} = \varepsilon_i \cdot \varepsilon_j - \frac{(p_i \cdot \varepsilon_j)(p_j \cdot \varepsilon_i)}{p_i \cdot p_j}. \quad (3.9)$$

where the $\{i, j, k\}$ in A_i are cyclic permutations of $\{1, 2, 3\}$. For form factors with two external gluons, there is only one gauge invariant basis $B_0 = C_{12}$.

Next we consider form factor containing external quarks. The amplitudes (form factors) with a pair of quark fields contains fermion chains structures like $\bar{u} \not{\epsilon} \not{p} \cdots u$. To define gauge invariant basis, we need to discriminate operators with even and odd number of gamma matrices, which will be denoted as O_{even} and O_{odd} , respectively. For example the operators $\bar{\psi}\psi$ and $F^{\mu\nu} \bar{\psi} \gamma_{\mu\nu} \psi$ belongs to O_{even} , while $F^{\mu\nu} D_\mu \bar{\psi} \gamma_\nu \psi$ belongs to O_{odd} . One major difference between O_{even} and O_{odd} is that in a Feynman diagram, if O_{even} appears in a fermion loop, the gamma trace of this fermion loop would contain odd number of gamma matrices, thus vanish. An example is shown in Figure 1. By contrast, a Feynman diagram with O_{odd} in the fermion loop does not vanish. The scattering amplitude, and consequently the gauge invariant basis, of O_{even} or O_{odd} contains product of even or odd number of gamma matrices, respectively.

Let us start with the gauge invariant basis of the $H \rightarrow q\bar{q}$ amplitude. The gauge invariant basis only contains a single element $B_1 = \bar{u}(p_2)u(p_1)$. Since the gauge invariant basis of O_{odd} must contain odd number of gamma matrices in the product, the $O_{\text{odd}} \rightarrow q\bar{q}$ amplitude must vanish. The gauge invariant basis for $H \rightarrow q\bar{q}$ can be summarized as:

$$B^{\text{odd}} = \{\}, \quad B^{\text{even}} = \{\bar{u}(p_2)u(p_1)\}. \quad (3.10)$$

The gauge invariant basis of $H \rightarrow q\bar{q}g$ amplitude contains 4 types of fermion contractions, $\bar{u}(p_2)u(p_1)$, $\bar{u}(p_2) \not{p}_3 u(p_1)$, $\bar{u}(p_2) \not{\epsilon}_3 u(p_1)$ and $\bar{u}(p_2) \not{\epsilon}_3 \not{p}_3 u(p_1)$, in which two of them contain odd/even number of gamma matrices. The gauge invariance basis can be constructed as:

$$B^{\text{odd}} = \{\bar{u}(p_2) \not{p}_3 u(p_1) A_3, \quad \bar{u}(p_2) \not{\epsilon}_3 u(p_1)(p_1 \cdot p_3) - \bar{u}(p_2) \not{p}_3 u(p_1)(p_1 \cdot \epsilon_3)\}, \quad (3.11)$$

$$B_1^{\text{even}} = \{\bar{u}(p_2)u(p_1) A_3, \quad \bar{u}(p_2) \not{\epsilon}_3 \not{p}_3 u(p_1)(p_1 \cdot p_3)\}. \quad (3.12)$$

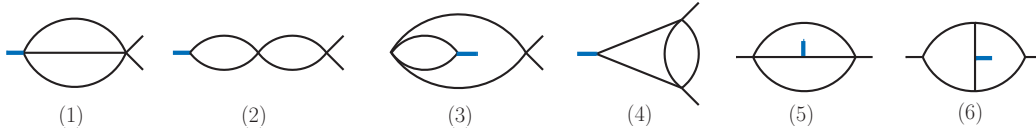


Figure 2. The master integrals of the 2-loop 2-point form factor.

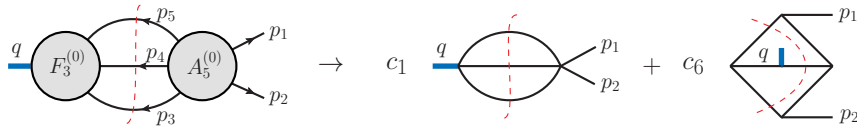


Figure 3. The triple cut for a two-loop form factor of $\text{tr}(F^2)$ with two external particles.

After expanding a form factor in the gauge invariant basis as in (3.5), the helicity information is contained in the basis B_α , and f_n^α contains only scalar product of loop and external momenta, which can be reduced directly using IBP. Comparing with other tensor reduction methods like the PV reduction, the gauge invariant basis method produces integrals with less numerator power, and the coefficients of the integrals are more compact and do not contain Gram determinants.

3.3 Planar unitarity cut

It is well known that it is much easier to evaluate the planar scattering amplitude, or the leading N_c order of the amplitude, than the non-planar contributions. In the case of form factors, we may still define the planar contributions as the leading N_c order of the form factor. Similar as scattering amplitudes, planar form factors can also be computed using planar unitarity cut, in which the tree building blocks are color stripped amplitudes. As will be shown in Sect. 4, we can even use the planar cut to compute the full color dependence of the two-loop three-gluon form factors.

An important difference between the planar form factor and the planar scattering amplitude is that the planar form factor contains integrals whose topologies are non-planar. This is because the operator (or the Higgs particle) is a color singlet, thus the presence of the operator does not alter the structure of the color diagram. So the diagram contributes to the leading N_c order even if the operator appears in the middle of the diagram. Similar as the planar diagrams of scattering amplitudes, the planar diagrams of form factors can also be embed on a disc, and the on-shell states are still positioned on the boundary cyclicly. However, the operator may appear in any position of the planar diagram. Since the operator carries a non-zero momentum q , the planar diagram for form factors may correspond to a non-planar integral.

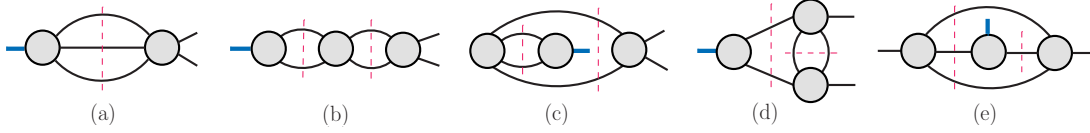


Figure 4. The cuts needed in the 2-loop 2-point form factor calculation.

Two-loop two-gluon form factor

As a simple example, we consider the two-point two-loop form factor in pure gluon sector. The complete set of master integrals are given in Figure 2. We demonstrated the planar unitarity cut by considering the triple-cut shown in the l.h.s. of Figure 3.

The building blocks of the cut are a planar three-gluon tree form factor and a planar five-gluon tree amplitudes:

$$\sum_{\text{helicities of } \varepsilon_{3,4,5}} F_3(-5, -4, -3) A_5(1, 2, 3, 4, 5). \quad (3.13)$$

The polarization vectors $\varepsilon_{3,4,5}$ of the cut gluons are summed using the contraction rule in (3.3), then the polarization vectors $\varepsilon_{1,2}$ of the external gluons are contracted with the gauge invariant basis, which contains a single element $B_0 = C_{12}$ in (3.9). Thus we have

$$\sum_{\text{helicities}} F_3 A_5 = [(\varepsilon_1 \cdot \varepsilon_2)(p_1 \cdot p_2) - (p_1 \cdot \varepsilon_2)(p_2 \cdot \varepsilon_1)] f_0(\{s_{ij}, D\}). \quad (3.14)$$

The scalar function f_0 is a function rational in s_{ij} and polynomial in the dimension parameter D , which can be directly reduced using IBP reduction with e.g. public codes [79–82]. As shown in the r.h.s. of Figure 3, only two master integrals (1) and (6) in Figure 2 enter in this cut. This cut allows us to compute their coefficients $\{c_1, c_6\}$:

$$c_1 = 12D - \frac{1175}{6(D-4)} - \frac{1}{D-3} + \frac{48}{D-2} + \frac{58}{9(D-1)} + \frac{525}{32(2D-7)} + \frac{107}{288(2D-5)} - \frac{694}{3(D-4)^2} - \frac{16}{(D-2)^2} - \frac{96}{(D-4)^3} - \frac{1955}{16}, \quad (3.15)$$

$$c_6 = \frac{3(D-3)(3D-8)}{4(2D-7)(2D-5)}, \quad (3.16)$$

which are consistent with the known result (see e.g. [83]).

To determine the coefficients of other master integrals, four other cuts can be used as shown in Figure 4. More explicitly: cut-(b) for $\{c_2\}$, cut-(c) for $\{c_3\}$, cut-(d) for $\{c_4\}$ and cut-(e) for $\{c_5, c_6\}$. Note that c_6 appears in both cut-(a) and (e), which provides a non-trivial consistency check.

The full form factor $\mathcal{F}_{\mathcal{O}_1}^{(2)}$ can be written as

$$\mathcal{F}_{\mathcal{O}_1}^{(2)}(p_1, p_2; q) = \left(\sum_{i=1}^4 c_i M_i + \frac{1}{2} \sum_{i=5,6} c_i M_i \right) + \text{perms}(p_1, p_2), \quad (3.17)$$

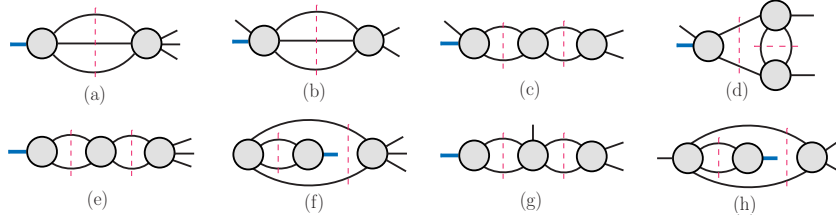


Figure 5. The cuts needed in the 2-loop 3-point form factor calculation.

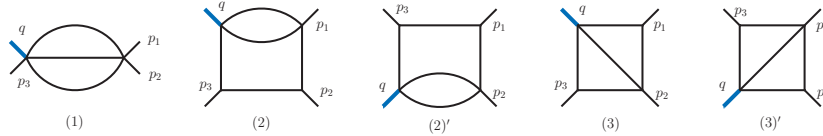


Figure 6. Master integrals of $\mathcal{F}_{\mathcal{O}_2}^{(2)}$ captured by the s_{12} triple cut (b) in Figure 5.

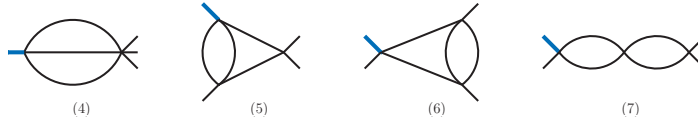


Figure 7. Master integrals of $\mathcal{F}_{\mathcal{O}_2}^{(2)}$ that are *not* captured by the triple cut (b) in Figure 5.

where M_i correspond to the master integrals with label (i) in Figure 2. Notice that the permutation of two external gluons does not alter the integrals (5) and (6), so for these two master integrals a factor $\frac{1}{2}$ is added to avoid double counting.

Two-loop three-gluon form factor

The set of cuts which is sufficient for the computation of the three-point two-loop form factors are given in Figure 5. All these cuts are all required for the length-2 operators, while for length-3 operators only the 4 cuts in the first row are needed. Consider the two-loop three-gluon form factor of length-3 operator \mathcal{O}_1 as an example. $\mathcal{F}_{\mathcal{O}_1}^{(2)}$ contains seven master integrals up to permutations of external legs, as show in Figure 6 and Figure 7. Each cut fixes the coefficients of a subset of these master integrals. For example, triple cut (b) of Figure 5 in s_{12} -channel determines the coefficients of five master integrals in Figure 6, and the coefficients of $(2)'$ (or $(3)'$) are related to that of (2) (or (3)) by flipping symmetry $p_1 \leftrightarrow p_2$. If a master integral appears in the result of several different cuts, its coefficient in these cuts must be the same. These provides consistency check for the computation.

For the Higgs to three-parton amplitudes considered in this paper, the full set of master integrals are shown in Fig. 8. They have been computed in terms of 2d harmonic polylogarithms [41, 84]. Using these expressions we can obtain the analytic bare form factors.

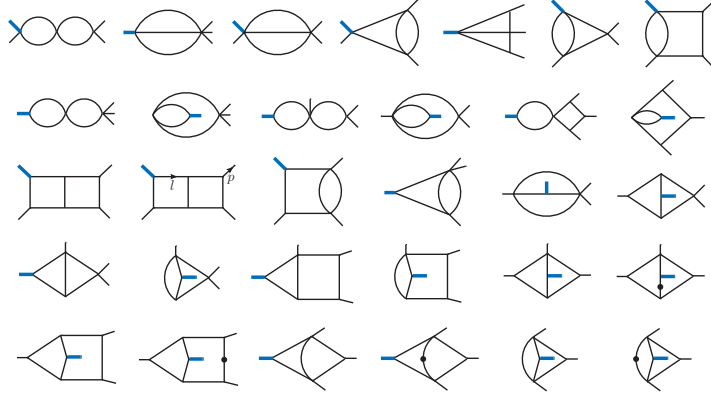


Figure 8. The full set of master integrals of the two-loop 3-point form factor. The line with a dot represents a double propagator.

4 Color decomposition of fermion cuts

In the pure gluon sector, planar cuts are enough to construct the full form factors. The cut form factor can be decomposed into several planar tree form factors or amplitudes. However, such a decomposition is not obvious in the presence of quark loops. In this section we show that, in the case of Higgs to 3-gluon amplitudes, by making connection between the fundamental and adjoint fermions, a nice color decomposition is still possible, such that the full 2-loop integrand can be constructed using planar cuts.

In our notation, gluons carry an adjoint color index $a = 1, 2, \dots, N_c^2 - 1$, and quarks and antiquarks carry an N_c or \bar{N}_c index, $i, \bar{j} = 1, \dots, N_c$. We will use the group algebras

$$\text{Tr}(T^a T^b) = t_F \delta^{ab}, \quad (T^a T^a)_i^{\bar{j}} = C_F \delta_i^{\bar{j}}, \quad (T^a T^b T^a)_i^{\bar{j}} = \left(C_F - \frac{C_A}{2}\right) (T^b)_i^{\bar{j}}. \quad (4.1)$$

We denote f_x for the flavor index of quarks and the contraction is given by $\delta_{f_x f_x} = n_f$.

4.1 Color decomposition of tree amplitudes

For the purpose of computing Higgs to 3-gluon amplitudes, we need tree amplitudes and form factor with quark pairs. As far as color factors are concerned, we do not need to discriminate amplitudes and color factors. Since the Higgs field is a color singlet, we can remove it from the form factor color graph, what is left is the color graph of a scattering amplitude. For example, the $H \rightarrow 3g$ tree form factor has the color factor f^{abc} , which is the same as the color factor of 3-gluon tree amplitude.

We use the following color decomposition of n -gluon tree amplitudes:

$$\mathcal{A}(1_g, 2_g, \dots, n_g) = \sum_{\sigma \in S_{n-2}} A\left((n-1)\sigma_1 \sigma_2 \dots \sigma_{n-2} n\right) f^{a_{n-1} a_{\sigma_1} \dots a_{\sigma_{n-2}} a_n}. \quad (4.2)$$

Here \mathcal{A} (\mathcal{F}) denotes the amplitude (form factors) with full color factors, while A (F) denotes the color stripped planar amplitude (form factors).

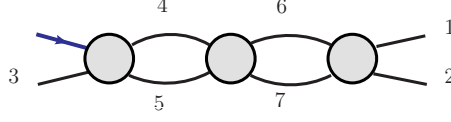


Figure 9. The s_{12} double bubble cut

For tree amplitudes with a quark pair and $(n - 2)$ gluons, a similar color decomposition is

$$\mathcal{A}(1_g, 2_g, 3_g, \dots, (n-1)_q, n_{\bar{q}}) = \sum_{\sigma \in S_{n-2}} A\left((n-1)_q \sigma(1) \dots \sigma(n-2) n_{\bar{q}}\right) (T^{a_{\sigma_1}} \dots T^{a_{\sigma_{n-2}}})_{i_{n-1}}^{\bar{i}_n} \delta_{f_1 f_n}. \quad (4.3)$$

The color decomposition of the 4-quark tree amplitude is

$$\mathcal{A}(1_q, 2_q, 3_{\bar{q}}, 4_{\bar{q}}) = A(1342)(T^a)_{i_1}^{\bar{i}_3}(T^a)_{i_2}^{\bar{i}_4} \delta_{f_1 f_3} \delta_{f_2 f_4} + A(1432)(T^a)_{i_1}^{\bar{i}_4}(T^a)_{i_2}^{\bar{i}_3} \delta_{f_1 f_4} \delta_{f_2 f_3}. \quad (4.4)$$

4.2 The s_{12} two double-cut

The s_{12} two double cut, as show in Figure 9, corresponds to the product of a 3-point form factor and two 4-point amplitudes, $\mathcal{F}(345)\mathcal{A}(7654)\mathcal{A}(1267)$.

First we consider the case when all cut lines (4, 5, 6, 7) are all fermions. The cut integrand is the product of the following three tree amplitudes,

$$\mathcal{F}(3_g, 4_{\bar{q}}, 5_q) = F(3_g, 4_{\bar{q}}, 5_q)(T^{a_3})_{i_5}^{\bar{i}_4} \delta_{f_5 f_4}, \quad (4.5)$$

$$\mathcal{A}(1_g, 2_g, 6_q, 7_{\bar{q}}) = \left[A(1_g, 2_g, 7_{\bar{q}}, 6_q)(T^{a_1} T^{a_2})_{i_6}^{\bar{i}_7} + A(2_g, 1_g, 7_{\bar{q}}, 6_q)(T^{a_2} T^{a_1})_{i_6}^{\bar{i}_7} \right] \delta_{f_6 f_7}, \quad (4.6)$$

$$\mathcal{A}(7_q, 6_{\bar{q}}, 5_{\bar{q}}, 4_q) = A(5_{\bar{q}}, 4_q, 7_q, 6_{\bar{q}})(T^a)_{i_4}^{\bar{i}_5}(T^a)_{i_7}^{\bar{i}_6} \delta_{f_4 f_5} \delta_{f_7 f_6} + (4 \leftrightarrow 7). \quad (4.7)$$

After contracting the color and flavor indices, the cut integrand can be reduced to

$$\mathcal{F}\Big|_{\text{cut}}^{qqqq} = F(3_g, 4_{\bar{q}}, 5_q) \left[A(5_{\bar{q}}, 4_q, 7_q, 6_{\bar{q}}) n_f^2 t_F + A(5_{\bar{q}}, 7_q, 4_q, 6_{\bar{q}}) \left(C_F - \frac{C_A}{2} \right) n_f \right] \\ \times \left[A(1_g, 2_g, 7_{\bar{q}}, 6_q) \text{Tr}(T^{a_1} T^{a_2} T^{a_3}) + A(2_g, 1_g, 7_{\bar{q}}, 6_q) \text{Tr}(T^{a_1} T^{a_3} T^{a_2}) \right]. \quad (4.8)$$

We can see that the product of tree amplitudes apparently do not have planar structure. Four different color structures appears in this configuration, and we rewrite (4.8) as

$$\mathcal{F}\Big|_{\text{cut}}^{qqqq} = \left[c_1 n_f^2 t_F + c_2 n_f (C_F - \frac{C_A}{2}) \right] \text{Tr}(T^{a_1} T^{a_2} T^{a_3}) \\ + \left[c_3 n_f^2 t_F + c_4 n_f (C_F - \frac{C_A}{2}) \right] \text{Tr}(T^{a_1} T^{a_3} T^{a_2}). \quad (4.9)$$

An important observation is that our discussion so far applies to general representation of quarks. In the case that quarks are in adjoint representation, it is clear that the cut integrand is proportional to $C_A^2 f^{a_1 a_2 a_3}$ and can be written as

$$\mathcal{F}_{\text{adj}}^{qqqq}\Big|_{\text{cut}} = (X_1 n_f^2 + X_2 n_f) C_A^2 f^{a_1 a_2 a_3}. \quad (4.10)$$

Also, in adjoint representation the cut integrand can be obtained from planar unitarity cut, and X_1 and X_2 correspond to the coefficients of n_f^2 and n_f in the planar cut integrand, respectively.

In order to match (4.9) and (4.10) when taking fermions to be adjoint, we must have $c_3 = -c_1$ and $c_4 = -c_2$, and (4.9) can be reduced to

$$\mathcal{F}\Big|_{\text{cut}}^{qqqq} = i \left[c_1 n_f^2 t_F + c_2 n_f (C_F - \frac{C_A}{2}) \right] t_F f^{a_1 a_2 a_3}. \quad (4.11)$$

Furthermore, in the adjoint fermion case, the two color factors above reduces to $t_F \rightarrow C_A$, $C_F - \frac{C_A}{2} \rightarrow \frac{C_A}{2}$. By matching the n_f^2 and n_f terms, the generic representation result can be written as

$$\mathcal{F}\Big|_{\text{cut}}^{qqqq} = \left[X_1 n_f^2 t_F^2 + X_2 n_f t_F (2C_A - C_F) \right] f^{a_1 a_2 a_3}. \quad (4.12)$$

So the cut integrand can be obtained using planar unitarity cut in the adjoint case. To be more explicit: first, one compute the cut integrand in the adjoint representation using planar unitarity cut, then replace C_A^2 by t_F^2 in the coefficient of n_f^2 , and replace C_A^2 by $t_f (C_A - \frac{C_F}{2})$ in the coefficient of n_f .

In the case that (4, 5) are gluons, and (6, 7) are fermions, one obtain the following color decomposition:

$$\begin{aligned} \mathcal{F}\Big|_{\text{cut}}^{ggqq} &= F(3_g, 4_g, 5_g) \frac{iC_A}{2} n_f t_F \left[A(4_g, 5_g, 6_{\bar{q}}, 7_q) - A(5_g, 4_g, 6_{\bar{q}}, 7_q) \right] \\ &\times \left[A(1_g, 2_g, 7_{\bar{q}}, 6_q) \text{Tr}(T^{a_1} T^{a_2} T^{a_3}) + A(2_g, 1_g, 7_{\bar{q}}, 6_q) \text{Tr}(T^{a_2} T^{a_1} T^{a_3}) \right], \end{aligned} \quad (4.13)$$

which has only two color structure, $C_A t_F \text{Tr}(T^{a_1} T^{a_2} T^{a_3})$ and $C_A t_F \text{Tr}(T^{a_1} T^{a_3} T^{a_2})$. The same structure happens in the case (4, 5) are fermions, and (6, 7) are gluons. By similar analysis as the previous example, if we denote the cut amplitude in adjoint representation as

$$\mathcal{F}_{\text{adj}}\Big|_{\text{cut}}^{ggqq} = X_3 n_f C_A^2 f^{a_1 a_2 a_3}, \quad \mathcal{F}_{\text{adj}}\Big|_{\text{cut}}^{qqgg} = X_4 n_f C_A^2 f^{a_1 a_2 a_3}, \quad (4.14)$$

the cut amplitude in generic representation can be written as

$$\mathcal{F}\Big|_{\text{cut}}^{ggqq} = X_3 n_f t_F C_A f^{a_1 a_2 a_3}, \quad \mathcal{F}\Big|_{\text{cut}}^{qqgg} = X_4 n_f t_F C_A f^{a_1 a_2 a_3}. \quad (4.15)$$

Here again, X_3 and X_4 can be extracted form the cut integrand in adjoint representation.

The above discussion means that, similar as in the adjoint representation, the planar cut is suffice to determine the s_{12} double 2-cut integrand in the generic representations. The only difference is that different color factors should be assigned to different terms in the cut integrand. All these color factors should be reduced to C_A^2 in the adjoint representation.

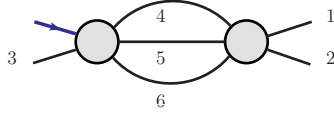


Figure 10. The s_{12} triple-cut

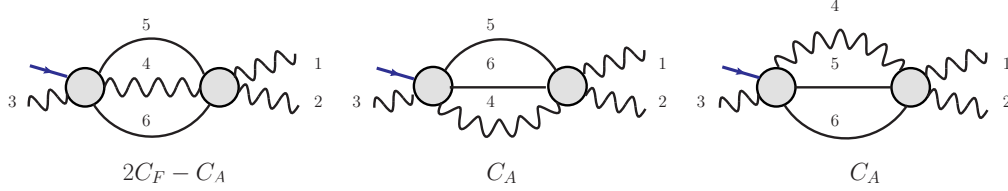


Figure 11. Different ordering of fields corresponds to different color factors.

4.3 The s_{12} triple-cut

The s_{12} triple cut corresponds to the product of a 4 point form factor and a 5 point amplitudes, $\mathcal{F}(3456)\mathcal{A}(12456)$, as show in Figure 10. If the internal states are all gluons, the color factor is C_A^2 , which is simple. Now consider the case $(4, 5, 6) = (g, q, \bar{q})$. The tree amplitudes are

$$\begin{aligned} \mathcal{F}(3_g, 4_g, 5_{\bar{q}}, 6_q) &= F(3_g, 4_g, 5_{\bar{q}}, 6_q)(T^{a_3}T^{a_4})_{i_6}^{\bar{i}_5} \delta_{f_6 f_5} + (3 \leftrightarrow 4), \\ \mathcal{A}(1_g, 2_g, 4_g, 5_q, 6_{\bar{q}}) &= A(1_g, 2_g, 4_g, 6_{\bar{q}}, 5_q)(T^{a_1}T^{a_2}T^{a_4})_{i_5}^{\bar{i}_6} \delta_{f_5 f_6} + \text{permutations of } (124). \end{aligned} \quad (4.16)$$

Contracting the color and flavor indices, and using the $U(1)$ decoupling relation

$$A(14265) = -A(12465) - A(12645) - A(12654), \quad (4.17)$$

the cut amplitude can be rewritten as

$$\begin{aligned} \mathcal{F}|_{\text{cut}}^{gqq} &= \frac{n_f}{2} \text{Tr}(T^{a_1}T^{a_2}T^{a_3}) \left[(2C_F - C_A)F(3546)A(12645) + C_A F(4356)A(12465) \right. \\ &\quad \left. + C_A F(3456)A(41265) \right] + (1 \leftrightarrow 2). \end{aligned} \quad (4.18)$$

The three terms in the bracket in (4.18) take obviously the planar-cut form and correspond to the three different internal-state configurations in Figure 11, respectively. If the gluon line appears in the middle of the diagram, the color factor is $2C_F - C_A$, otherwise it is C_A . The same pattern also appears in other cuts.

4.4 Other cuts

Following the same steps as in the last two subsections, the color structures of the other cuts can be computed, and it turns out that for every cut, a color decomposition is possible. We summarize all cases as follows (where (a)-(h) correspond to labels in Fig. 6):

1. s_{123} two double-cut (e)-(f): both planar and non-planar cases have factor C_F .

Table 1. Notation of form factors with three partons, where \pm indicates position or negative helicity gluons.

external particles	$(1^-, 2^-, 3^-)$	$(1^-, 2^-, 3^+)$	$(1^q, 2^{\bar{q}}, 3^-)$
form factors	$\mathcal{F}_{\mathcal{O}_i, \alpha}^{(l)}$	$\mathcal{F}_{\mathcal{O}_i, \beta}^{(l)}$	$\mathcal{F}_{\mathcal{O}_i, \gamma}^{(l)}$

2. s_{12} two double-cut (c): 4 fermion cut, $n_f(2C_F - C_A)$ and $n_f^2 t_F$. Other channels C_A .
3. s_{123} triple-cut (a), s_{12} triple-cut (b), s_{12} triangle-bubble-cut (d): Diagrams in which gluon appears in the middle have factor $2C_F - C_A$. Other channels have factor C_A .
4. $s_{12} - s_{123}$ two double-cut (g)-(h): the nonplanar case has factor $2C_F - C_A$, the planar case has factor C_A .

These allow us to compute full amplitudes using only planar cuts.

5 Results

In this section we perform renormalization and IR subtraction for form factors and obtain compact analytic forms. The two-loop bare form factor contains UV and IR divergences as discussed in Sect. 2.2. The $1/\epsilon^m$, $m = 4, 3, 2$ pole terms must cancel with the universal IR divergence and the 1 loop UV divergence, which offers non-trivial self-consistency check of the results. The cancellation of $1/\epsilon$ pole term then determines the two-loop anomalous dimension of the operator.

As an important check of the method, we have reproduced known results including the non-trivial two-loop amplitudes of Higgs to three partons with the operator $\text{tr}(F^2)$ [27]. As a further check, we recall that the form factors should satisfy the linear relation (2.8). We compute form factors of different operators independently. We explicitly check that, already at the level of IBP master integrals, the results satisfy exactly this linear relation. This provides a strong consistency check for our computation. We would like to emphasize the computation of form factors of $\text{tr}(D^2 F^2)$ is more involving than the known result of $\text{tr}(F^2)$ due to extra derivatives in the operator, and our method can be efficiently applied to such case as well as operators with higher dimension.

A word about notation: for form factors with three partons, it is enough to consider three configurations given in Table 1. We use subindices α, β, γ to denote different external states, similar to that in [27]. We introduce dimensionless variables:

$$u = \frac{s_{12}}{s_{123}}, \quad v = \frac{s_{23}}{s_{123}}, \quad w = \frac{s_{13}}{s_{123}}, \quad \text{where } s_{123} = q^2 = m_H^2. \quad (5.1)$$

Table 2. Normalized tree-level form factors $r_{\hat{\mathcal{O}}_I}^{(0)} = \mathcal{F}_{\hat{\mathcal{O}}_I}^{(0)} / \mathcal{F}_{\hat{\mathcal{O}}_2}^{(0)}$.

$r_{\hat{\mathcal{O}}}^{(0)}$	α	β	γ
$\hat{\mathcal{O}}_1$	$u v w$	0	0
$\hat{\mathcal{O}}_2$	1	1	1
$\hat{\mathcal{O}}_3$	0	0	0
$\hat{\mathcal{O}}_4$	0	0	u

5.1 Tree-level results

We first give the tree-level form factors for the dimension-5 operator [85]:

$$\mathcal{F}_{\mathcal{O}_0, \alpha}^{(0)} = \frac{s_{123}^2}{[12][23][31]}, \quad \mathcal{F}_{\mathcal{O}_0, \beta}^{(0)} = \frac{\langle 12 \rangle^4}{\langle 12 \rangle \langle 23 \rangle \langle 31 \rangle}, \quad \mathcal{F}_{\mathcal{O}_0, \gamma}^{(0)} = \frac{\langle 23 \rangle^2}{\langle 12 \rangle}. \quad (5.2)$$

Since the operators satisfy the linear relation (2.7), it is convenient to introduce $\hat{\mathcal{O}}_2$ as

$$\hat{\mathcal{O}}_2 \equiv \partial^2 \mathcal{O}_0. \quad (5.3)$$

The form factor of $\hat{\mathcal{O}}_2$ is the same as \mathcal{O}_0 up to an over all factor s_{123} :

$$\mathcal{F}_{\hat{\mathcal{O}}_2} = s_{123} \mathcal{F}_{\mathcal{O}_0}. \quad (5.4)$$

For convenience, we renormalize form factors by dividing the tree form factor of $\hat{\mathcal{O}}_2$ and introduce the ‘dimensionless’ form factors $r_{\hat{\mathcal{O}}_I}^{(\ell)}$ as

$$r_{\hat{\mathcal{O}}_I}^{(\ell)} := \mathcal{F}_{b, \hat{\mathcal{O}}_I}^{(\ell)} / \mathcal{F}_{\hat{\mathcal{O}}_2}^{(0)}, \quad (5.5)$$

The ratio tree-level form factors are given as (also summarized in Tab. 2):

$$r_{\hat{\mathcal{O}}_1, \alpha}^{(0)} = u v w, \quad r_{\hat{\mathcal{O}}_1, \beta}^{(0)} = r_{\hat{\mathcal{O}}_1, \gamma}^{(0)} = 0, \quad (5.6)$$

$$r_{\hat{\mathcal{O}}_3, \alpha}^{(0)} = r_{\hat{\mathcal{O}}_3, \beta}^{(0)} = r_{\hat{\mathcal{O}}_3, \gamma}^{(0)} = 0, \quad (5.7)$$

$$r_{\hat{\mathcal{O}}_4, \alpha}^{(0)} = r_{\hat{\mathcal{O}}_4, \beta}^{(0)} = 0, \quad r_{\hat{\mathcal{O}}_4, \gamma}^{(0)} = u. \quad (5.8)$$

Note that, we have normalized the operators $\{\hat{\mathcal{O}}_1, \hat{\mathcal{O}}_3, \hat{\mathcal{O}}_4\}$ properly, such that the 3-point tree form factors all have unit constant. From now on, we will take $\hat{\mathcal{O}}_I$ as the basis of dimension-6 operators:

$$\hat{\mathcal{O}}_I = \{\hat{\mathcal{O}}_1, \hat{\mathcal{O}}_2, \hat{\mathcal{O}}_3, \hat{\mathcal{O}}_4\}. \quad (5.9)$$

5.2 Loop corrections

We consider the form factors of \mathcal{O}_0 and $\hat{\mathcal{O}}_1$ in details. Explicit formulas and the results of other operators are collected in Appendix A – D.

Example 1: $\mathcal{F}_{\mathcal{O}_0}(1^-, 2^-, 3^-)$

We first consider the form factor of \mathcal{O}_0 and three gluons. This result has been obtained in [27]. The main purpose of this discussion is to make contact with the known literature and to set up the notation which will be used for the higher dimension operator cases. Since \mathcal{O}_0 is a length-2 operator, we have $\delta_n = 3 - 2 = 1$, defined in Sect. 2.2.

One-loop bare form factor is:

$$\mathcal{F}_{b, \mathcal{O}_0, \alpha}^{(1)} = \mathcal{F}_{\mathcal{O}_0, \alpha}^{(0)} \left(a_1 I_4[1, 2, 3, q] + b_1 I_2[s_{12}] + c_1 I_2[s_{123}] + (\text{cyclic perm.}) \right), \quad (5.10)$$

where I_4 and I_2 are one-loop box and bubble master integrals, and the master coefficients to all order in ϵ are

$$a_1 = \frac{u^2 v^2}{2w} \frac{\epsilon^2}{(2\epsilon - 1)} - \frac{uv}{2}, \quad (5.11)$$

$$b_1 = -n_f \frac{vw\epsilon}{(2\epsilon - 3)(\epsilon - 1)} + u\epsilon \left(\frac{v}{w} + \frac{w}{v} + \frac{\epsilon}{1 - \epsilon} \right) + \frac{vw\epsilon}{3 - 2\epsilon} + \frac{1}{\epsilon} - 2, \quad (5.12)$$

$$c_1 = \frac{1}{3}\epsilon \left(-\frac{vw}{u} - \frac{uv}{w} - \frac{uw}{v} + 3 \right) + \frac{1}{\epsilon - 1} - \frac{1}{\epsilon} + 3. \quad (5.13)$$

As discussed in Sect. 2.2, the renormalized one-loop form factor satisfies the following relation (with $\delta_n = 1$):

$$\mathcal{F}^{(1)} = S_\epsilon^{-1} \mathcal{F}_b^{(1)} + \left(Z^{(1)} - \frac{\beta_0}{2\epsilon} \right) \mathcal{F}_b^{(0)} = I^{(1)}(\epsilon) \mathcal{F}^{(0)} + \mathcal{F}^{(1), \text{fin}} + \mathcal{O}(\epsilon). \quad (5.14)$$

Using the bare one-loop form factor and universal IR information, we can extract the one-loop renormalization constant

$$Z_{\mathcal{O}_0}^{(1)} = -\frac{1}{\epsilon} \left(\frac{11C_A}{3} - \frac{2n_f}{3} \right) = -\frac{\beta_0}{\epsilon}. \quad (5.15)$$

The one-loop finite remainder can be obtained as

$$\mathcal{F}_{\mathcal{O}_0, \alpha}^{(1), \text{fin}} = \mathcal{F}_{\mathcal{O}_0, \alpha}^{(0)} \left(N_c \mathcal{R}_{\mathcal{O}_0, \alpha}^{(1), N_c} + n_f \mathcal{R}_{\mathcal{O}_0, \alpha}^{(1), n_f} \right), \quad (5.16)$$

where

$$\begin{aligned} \mathcal{R}_{\mathcal{O}_0, \alpha}^{(1), N_c} = & -2\text{Li}_2(1 - u) - 2\text{Li}_2(1 - v) - 2\text{Li}_2(1 - w) - \frac{11}{6} \log(uvw) + \frac{uv}{3} - \log(u) \log(v) \\ & + \frac{uw}{3} - \log(u) \log(w) + \frac{vw}{3} - \log(v) \log(w) + \frac{\pi^2}{2} - \frac{11 \log(-q^2)}{2}, \end{aligned} \quad (5.17)$$

$$\mathcal{R}_{\mathcal{O}_0, \alpha}^{(1), n_f} = \frac{1}{3} \log(uvw) - \frac{uv}{3} - \frac{uw}{3} - \frac{vw}{3} + \log(-q^2). \quad (5.18)$$

Similarly, the renormalized two-loop form factor satisfies the relation:

$$\begin{aligned} \mathcal{F}^{(2)} = & S_\epsilon^{-2} \mathcal{F}_b^{(2)} + S_\epsilon^{-1} \left[Z^{(1)} - \frac{3\beta_0}{2\epsilon} \right] \mathcal{F}_b^{(1)} + \left[Z^{(2)} - \frac{\beta_0}{2\epsilon} Z^{(1)} + \frac{3\beta_0^2}{8\epsilon^2} - \frac{\beta_1}{4\epsilon} \right] \mathcal{F}_b^{(0)} \\ = & I^{(2)}(\epsilon) \mathcal{F}^{(0)} + I^{(1)}(\epsilon) \mathcal{F}^{(1)} + \mathcal{F}^{(2), \text{fin}} + \mathcal{O}(\epsilon). \end{aligned} \quad (5.19)$$

Evaluating the bare two-loop form factor and using the universal IR information and one-loop results, we can extract the two-loop renormalization constant. The $1/\epsilon^2$ part is determined by the one-loop data as in (2.17), while the $1/\epsilon$ part is

$$Z_{\mathcal{O}_0}^{(2)} \Big|_{\frac{1}{\epsilon}\text{-part.}} = -\frac{1}{\epsilon} \left(\frac{34C_A^2}{3} - \frac{10C_A n_f}{3} - 2C_F n_f \right) = -\frac{\beta_1}{\epsilon}. \quad (5.20)$$

The two-loop finite remainder can be decomposed according to the color factors as

$$r_{\mathcal{O}_0, \alpha}^{(2), \text{fin}} = N_c^2 \mathcal{R}_{\mathcal{O}_0, \alpha}^{(2), N_c^2} + N_c n_f \mathcal{R}_{\mathcal{O}_0, \alpha}^{(2), N_c n_f} + \frac{n_f}{N_c} \mathcal{R}_{\mathcal{O}_0, \alpha}^{(2), n_f/N_c} + n_f^2 \mathcal{R}_{\mathcal{O}_0, \alpha}^{(2), n_f^2}. \quad (5.21)$$

The explicit expressions are given in [27] (see also [86]), which we do not reproduce here.³

Example 2: $\mathcal{F}_{\hat{\mathcal{O}}_1}(1^-, 2^-, 3^-)$

Next we consider the form factor of $\hat{\mathcal{O}}_1$. Since $\hat{\mathcal{O}}_1$ is a length-3 operator, we have $\delta_n = 3-3 = 0$. The one-loop bare form factor is given in terms of bubble integrals:

$$\mathcal{F}_{b, \hat{\mathcal{O}}_1, \alpha}^{(1)} = \mathcal{F}_{\hat{\mathcal{O}}_1, \alpha}^{(0)} \frac{-6 + 10\epsilon - 4\epsilon^2 - \epsilon^3}{2\epsilon(1-\epsilon)(3-2\epsilon)} (I_2[s_{12}] + I_2[s_{23}] + I_2[s_{13}]). \quad (5.22)$$

The renormalized one-loop form factor satisfies (with $\delta_n = 0$)

$$\mathcal{F}^{(1)} = S_\epsilon^{-1} \mathcal{F}_b^{(1)} + Z^{(1)} \mathcal{F}_b^{(0)} = I^{(1)}(\epsilon) \mathcal{F}^{(0)} + \mathcal{F}^{(1), \text{fin}} + \mathcal{O}(\epsilon), \quad (5.23)$$

from which we extract the one-loop renormalization constant

$$Z_{\hat{\mathcal{O}}_1}^{(1)} = \frac{1}{\epsilon} \left(\frac{C_A}{2} + n_f \right). \quad (5.24)$$

The renormalized two-loop form factor, using (2.21) with $\delta_n = 0$, satisfies

$$\begin{aligned} \mathcal{F}^{(2)} &= S_\epsilon^{-2} \mathcal{F}_b^{(2)} + S_\epsilon^{-1} \left[Z^{(1)} - \frac{\beta_0}{\epsilon} \right] \mathcal{F}_b^{(1)} + Z^{(2)} \mathcal{F}_b^{(0)} \\ &= I^{(2)}(\epsilon) \mathcal{F}^{(0)} + I^{(1)}(\epsilon) \mathcal{F}^{(1)} + \mathcal{F}^{(2), \text{fin}} + \mathcal{O}(\epsilon). \end{aligned} \quad (5.25)$$

The cancellation of divergence fixes the two-loop renormalization constant. The $1/\epsilon^2$ part is determined by the one-loop data as in (2.17), while the $1/\epsilon$ part presents interesting new structure of operator mixing:

$$(Z^{(2)})_1^J \times r_{\hat{\mathcal{O}}_J, \alpha}^{(0)} \Big|_{\frac{1}{\epsilon}\text{-part.}} = \frac{1}{\epsilon} \left(\frac{25N_c^2}{12} + \frac{5N_c n_f}{12} - \frac{3n_f}{4N_c} \right) r_{\hat{\mathcal{O}}_1, \alpha}^{(0)} - \frac{1}{\epsilon} N_c^2 r_{\hat{\mathcal{O}}_2, \alpha}^{(0)}. \quad (5.26)$$

We can see that the first term provides a diagonal part of the renormalization constant matrix:

$$(Z^{(2)})_1^1 \Big|_{\frac{1}{\epsilon}\text{-part.}} = \frac{1}{\epsilon} \left(\frac{25N_c^2}{12} + \frac{5N_c n_f}{12} - \frac{3n_f}{4N_c} \right), \quad (5.27)$$

³In our notation, $r_{\mathcal{O}_0}^{(2), \text{fin}}$ corresponds to $\Omega^{(2), \text{finite}}$ in [27].

while the second term is due to the mixing with $\hat{\mathcal{O}}_2$ which gives an off-diagonal component:

$$(Z^{(2)})_1^2 = -\frac{1}{\epsilon} N_c^2. \quad (5.28)$$

The two-loop finite remainder can be further simplified using Symbol techniques [87]. We decompose it according to the color factors as

$$\mathcal{F}_{\hat{\mathcal{O}}_1, \alpha}^{(2), \text{fin}} = \mathcal{F}_{\hat{\mathcal{O}}_1}^{(0)} \left(N_c^2 \mathcal{R}_{\hat{\mathcal{O}}_1, \alpha}^{(2), N_c^2} + N_c n_f \mathcal{R}_{\hat{\mathcal{O}}_1, \alpha}^{(2), N_c n_f} + n_f^2 \mathcal{R}_{\hat{\mathcal{O}}_1, \alpha}^{(2), n_f^2} + \mathcal{R}_{\hat{\mathcal{O}}_1, \alpha; \log(-q^2)}^{(2)} \right), \quad (5.29)$$

where the explicit expressions are collected in Appendix B.

Form factors of other operators and other external states can be obtained following the same procedure. Similar operator mixing effect also appears in other form factors, and we summarize the renormalization matrix in Sect. 5.3. The one-loop results in master expansion are collected in Appendix A. The two-loop finite remainders are collected in Appendix B – D.

5.3 Operator mixing

As discussed above in (5.26), the operators in general have operator mixing effects, represented by the renormalization constant matrix Z_I^J defined through

$$\hat{\mathcal{O}}_I^{\text{Ren}} = Z_I^J \hat{\mathcal{O}}_J^{\text{Bare}}. \quad (5.30)$$

We summarize below the renormalization constant matrix for dimension-6 operators at one and two loops.

At one-loop, there is no operator mixing since the renormalization constant matrix is diagonal:

$$(Z_{\hat{\mathcal{O}}}^{(1)}) = \frac{1}{\epsilon} \begin{pmatrix} \frac{N_c}{2} + n_f & 0 & 0 & 0 \\ 0 & -\beta_0 & 0 & 0 \\ 0 & 0 & (Z^{(1)})_3^3 & 0 \\ 0 & 0 & 0 & \frac{8C_F}{3} + \frac{2n_f}{3} \end{pmatrix}.$$

Two-loop renormalization $Z^{(2)}$ contains $1/\epsilon^2$ pole terms which are determined by the one-loop matrix using (2.17). The simple pole term is the intrinsic new two-loop contribution:

$$(Z_{\hat{\mathcal{O}}}^{(2)}) \Big|_{\frac{1}{\epsilon}\text{-part.}} = \quad (5.31)$$

$$\frac{1}{\epsilon} \begin{pmatrix} \frac{25N_c^2}{12} + \frac{5N_c n_f}{12} - \frac{3n_f}{4N_c} & -N_c^2 & (Z^{(2)})_1^3 & \frac{5}{9} + \frac{5N_c^2}{12} \\ 0 & -\beta_1 & 0 & 0 \\ 0 & 0 & (Z^{(2)})_3^3 & n_f \left(\frac{5N_c}{72} + \frac{1}{18N_c} \right) + \frac{1}{36} + \frac{7}{72N_c^2} \\ 0 & \left(-\frac{5N_c}{6} + \frac{2}{9N_c} \right) n_f & (Z^{(2)})_4^3 & \frac{80N_c^2}{27} - \frac{20}{9} + \frac{7}{27N_c^2} + \left(\frac{25N_c}{27} + \frac{13}{18N_c} \right) n_f \end{pmatrix}.$$

To determine the matrix elements $(Z^{(l)})_I^3$, one needs to compute form factors of $\hat{\mathcal{O}}_3$ with four partons, which we leave for future work.

6 Discussion

The results in last section provide the complete two-loop QCD corrections to Higgs plus 3-parton amplitudes with dimension-7 operators. These amplitudes are of phenomenological relevance for the LHC experiments, which provide for the first time the top-mass correction of S-matrix elements for Higgs plus one-jet production at N²LO. A result with full top-mass dependence would require a three-loop computation involving a massive subloop, which is beyond the state of the art. Our computation relies on a combination of modern on-shell unitarity-cut method and IBP reduction. This strategy can be applied efficiently to the case with higher dimension operators in the Higgs effective action.

The analytic results take remarkable simple form and exhibits intriguing hidden structures. Below we comment on this in more details. First of all, the maximally transcendental part takes universal forms, generalizing the so-call maximal transcendentality principle and showing a direct connection between QCD and $\mathcal{N} = 4$ SYM. The generalization is in two aspects. Firstly, the maximal transcendentality principle applies to Higgs to three-parton amplitudes (or form factors) with high dimension operators, see also [52–56]. Secondly, as also discussed in [56], the principle applies also to Higgs amplitudes with external quark states, by a change of color factors:

$$\text{Max. Tran. of } (H \rightarrow q\bar{q}g) \Big|_{C_F \rightarrow C_A} = \text{Max. Tran. of } (H \rightarrow 3g). \quad (6.1)$$

For example, for length-3 operators such as \mathcal{O}_1 and \mathcal{O}_4 , the maximal transcendentality part are related to the following universal function:⁴

$$\begin{aligned} R_{L3;4}^{(2)}(u, v, w) := & -\frac{3}{2}\text{Li}_4(u) + \frac{3}{4}\text{Li}_4\left(-\frac{uv}{w}\right) - \frac{3}{4}\log(w) \left[\text{Li}_3\left(-\frac{u}{v}\right) + \text{Li}_3\left(-\frac{v}{u}\right) \right] \\ & + \frac{\log^2(u)}{32} [\log^2(u) + \log^2(v) + \log^2(w) - 4\log(v)\log(w)] \\ & + \frac{\zeta_2}{8} [5\log^2(u) - 2\log(v)\log(w)] - \frac{1}{4}\zeta_4 + \text{perms}(u, v, w), \end{aligned} \quad (6.2)$$

and the results in (B.3) and (D.13) satisfy

$$\mathcal{R}_{\hat{\mathcal{O}}_1, \alpha; 4}^{(2)} = R_{L3;4}^{(2)}(u, v, w) = \mathcal{R}_{\hat{\mathcal{O}}_4; \gamma; 4}^{(2), N_c^2} - \mathcal{R}_{\hat{\mathcal{O}}_4; \gamma; 4}^{(2), N_c^0} + \mathcal{R}_{\hat{\mathcal{O}}_4; \gamma; 4}^{(2), 1/N_c^{-2}}. \quad (6.3)$$

Note that the last equality exactly corresponds to taking $C_F \rightarrow C_A$. Physically, such an identification corresponds to changing the fermions from fundamental to adjoint representation. This has been known for the kinematic independent quantities such as anomalous dimensions [38, 39]. For pseudo-scalar Higgs amplitudes involving $q\bar{q}g$ states, the universal maximally transcendental part was also noted in [89].

⁴Since this is computed using Catani IR subtraction scheme, it is different (by purely the choice of IR subtraction scheme) from the expression in [52] as well as appeared in other form factors in $\mathcal{N} = 4$ SYM [44–47], which are based on the BDS subtraction scheme [88].

Even more intriguingly, the sub-leading transcendentality parts also show universal structures and have certain connections to that of $\mathcal{N} = 4$ SYM. The universal building block of transcendentality degree-3 part is:

$$\begin{aligned}
T_3(u, v, w) := & \left[-\text{Li}_3\left(-\frac{u}{w}\right) + \log(u)\text{Li}_2\left(\frac{v}{1-u}\right) - \frac{1}{2}\log(1-u)\log\left(\frac{w^2}{1-u}\right) \right. \\
& + \frac{1}{2}\text{Li}_3\left(-\frac{uv}{w}\right) + \frac{1}{2}\log(u)\log(v)\log(w) + \frac{1}{12}\log^3(w) + (u \leftrightarrow v) \left. \right] \\
& + \text{Li}_3(1-v) - \text{Li}_3(u) + \frac{1}{2}\log^2(v)\log\left(\frac{1-v}{u}\right) - \zeta_2 \log\left(\frac{uv}{w}\right). \quad (6.4)
\end{aligned}$$

This T_3 function also appeared as building blocks in the $\mathcal{N} = 4$ form factors [45, 47, 52]. In our QCD results, all degree-3 parts can be express in terms of T_3 functions, plus simple ζ_3 or $(\zeta_2 \times \log)$ terms.

For transcendentality degree-2 part, a universal building block is:

$$T_2(u, v) := \text{Li}_2(1-u) + \text{Li}_2(1-v) + \log(u)\log(v) - \zeta_2, \quad (6.5)$$

We note that in [90], a similar transcendentality-two building block was found as

$$I_{123;45} = \text{Li}_2\left(1 - \frac{s_{12}}{s_{123}}\right) + \text{Li}_2\left(1 - \frac{s_{23}}{s_{123}}\right) + \log^2\left(\frac{s_{12}}{s_{23}}\right) + \zeta_2, \quad (6.6)$$

which is the finite part of one-mass box functions. This is very similar to our degree-2 building block (6.5).

As it is well-known that, the amplitude of $\mathcal{N} = 4$ SYM is relatively easy to calculate, while the calculation of QCD amplitude is much more difficult. The principle allows one to obtain part of a very difficult amplitude from a simpler amplitude which may be computed to very high loops. One should note that there are known examples where the maximal transcendentality principle does not apply. For example, MTP does not always hold for the four-gluon and five-gluon scattering amplitudes. The QCD four-gluon amplitudes contains polylogarithm functions, while $\mathcal{N} = 4$ SYM amplitudes only contain the simple log function. Counter examples were also noted in the Regge limit of amplitudes [91] and for form factor of stress tensor operator [92]. By now the sphere of application of MTP is still not clear. It would be interesting to explore the underlying mechanism and also consider more examples. Furthermore, it would be important to study further the structure of lower transcendentality parts which are needed for computing full QCD results. It would be worthy to consider amplitudes in $\mathcal{N} = 1, 2$ SYM, which may serve as bridges connecting the QCD and $\mathcal{N} = 4$ SYM amplitudes.

When scattering amplitudes are classified by the transcendental degrees, usually $\frac{1}{s^k}$ type spurious poles appear. The cancellation of these unphysical poles links terms with different transcendental degrees, and may be used to constrain the lower transcendentality parts of the amplitude from the higher transcendentality pieces. The analytical expressions of a subset of two-loop non-planar master integrals form Higgs to 3 parton amplitude with finite top quark

was obtained recently [93] (which corresponding NLO order in the Higgs EFT expansion). These integrals contains elliptical sectors. It would be interesting to explore whether there are universal analytical structures in the elliptical sectors.

Acknowledgments

It is a pleasure to thank Lance Dixon, Bo Feng, Hui Luo, Jian-Ping Ma, Ke Ren and Li Lin Yang for discussions. This work is supported in part by the National Natural Science Foundation of China (Grants No. 11822508, 11847612), by the Chinese Academy of Sciences (CAS) Hundred-Talent Program, and by the Key Research Program of Frontier Sciences of CAS. We also thank the support of the HPC Cluster of ITP-CAS.

A One-loop results

We provide the one-loop bare form factor results to all order in ϵ . The higher order in ϵ expansion will be needed in the higher loop computation. $r^{(l)}$ is the normalized form factor defined in (5.5). We have:

$$r_{b,\hat{\mathcal{O}}_1,\alpha}^{(1)} = uvwN_c \frac{-6 + 10\epsilon - 4\epsilon^2 - \epsilon^3}{2\epsilon(1-\epsilon)(3-2\epsilon)} (I_2[s_{12}] + I_2[s_{23}] + I_2[s_{13}]), \quad (\text{A.1})$$

$$r_{b,\hat{\mathcal{O}}_4,\alpha}^{(1)} = -uvwn_f \frac{\epsilon}{(1-\epsilon)(3-2\epsilon)} (I_2[s_{12}] + I_2[s_{23}] + I_2[s_{13}]), \quad (\text{A.2})$$

$$r_{b,\hat{\mathcal{O}}_1,\beta}^{(1)} = -\frac{vw}{u} N_c \frac{\epsilon^2}{2(1-\epsilon)(3-2\epsilon)} I_2[s_{12}], \quad (\text{A.3})$$

$$r_{b,\hat{\mathcal{O}}_4,\beta}^{(1)} = -\frac{vw}{u} n_f \frac{\epsilon}{(1-\epsilon)(3-2\epsilon)} I_2[s_{12}], \quad (\text{A.4})$$

$$r_{b,\hat{\mathcal{O}}_1,\gamma}^{(1)} = -uN_c \frac{\epsilon}{4(1-\epsilon)(3-2\epsilon)} I_2[s_{12}], \quad (\text{A.5})$$

$$\begin{aligned} r_{b,\hat{\mathcal{O}}_4,\gamma}^{(1)} = & u \left[\frac{(2\epsilon^2 - \epsilon + 2)}{4\epsilon N_c} - \frac{(1-\epsilon)n_f}{3-2\epsilon} \right] I_2[s_{12}] \\ & + u \left[\frac{(5\epsilon^3 - 9\epsilon^2 + 2\epsilon)}{4(3-2\epsilon)(1-\epsilon)\epsilon N_c} + \frac{(5\epsilon^3 - 12\epsilon^2 + 11\epsilon - 6) N_c}{4(3-2\epsilon)(1-\epsilon)\epsilon} \right] I_2[s_{13}] \\ & + u \left[\frac{N_c (-2u\epsilon^2 + v\epsilon^4 + v\epsilon^3 - 14v\epsilon^2 + 16v\epsilon - 6v - w\epsilon^3 - w\epsilon^2 + \epsilon^4)}{4v(3-2\epsilon)(1-\epsilon)\epsilon} \right. \\ & \left. + \frac{(-u\epsilon^3 - u\epsilon^2 + v\epsilon^4 + v\epsilon^3 - 10v\epsilon^2 + 6v\epsilon - 2w\epsilon^2 + \epsilon^4)}{4v(3-2\epsilon)(1-\epsilon)\epsilon N_c} \right] I_2[s_{23}], \quad (\text{A.6}) \end{aligned}$$

$$r_{b,\hat{\mathcal{O}}_3,\alpha}^{(1)} = r_{b,\hat{\mathcal{O}}_3,\beta}^{(1)} = r_{b,\hat{\mathcal{O}}_3,\gamma}^{(1)} = 0. \quad (\text{A.7})$$

B Two-loop remainder of $F_{\hat{\mathcal{O}}_1}$

In this and following appendices, we collect the two-loop remainder functions. We follow the definition of $r^{(l)}$ in (5.5).

B.1 $\hat{\mathcal{O}}_1 \rightarrow (1^-, 2^-, 3^-)$

The two-loop finite remainder can be decomposed according to the color factors as:

$$r_{\hat{\mathcal{O}}_1, \alpha}^{(2), \text{fin}} = r_{\hat{\mathcal{O}}_1}^{(0)} \left(N_c^2 \mathcal{R}_{\hat{\mathcal{O}}_1, \alpha}^{(2), N_c^2} + N_c n_f \mathcal{R}_{\hat{\mathcal{O}}_1, \alpha}^{(2), N_c n_f} + n_f^2 \mathcal{R}_{\hat{\mathcal{O}}_1, \alpha}^{(2), n_f^2} + \mathcal{R}_{\hat{\mathcal{O}}_1, \alpha; \log(-q^2)}^{(2)} \right), \quad (\text{B.1})$$

in which we separate the terms proportional to $\log(-q^2)$ in $\mathcal{R}_{\hat{\mathcal{O}}_1, \alpha; \log(q^2)}^{(2)}$.

We decompose the $\mathcal{R}_{\hat{\mathcal{O}}_1, \alpha}^{(2), N_c^2}$ part according to transcendentality degree d as

$$\mathcal{R}_{\hat{\mathcal{O}}_1, \alpha}^{(2), N_c^2} = \sum_{d=0}^4 \mathcal{R}_{\hat{\mathcal{O}}_1, \alpha; d}^{(2), N_c^2}, \quad (\text{B.2})$$

where

$$\mathcal{R}_{\hat{\mathcal{O}}_1, \alpha; 4}^{(2), N_c^2} = R_{\text{L3;4}}^{(2)}(u, v, w), \quad (\text{B.3})$$

$$\mathcal{R}_{\hat{\mathcal{O}}_1, \alpha; 3}^{(2), N_c^2} = \left(1 + \frac{u}{w} \right) T_3(u, v, w) + \frac{143}{72} \zeta_3 - \frac{11}{24} \zeta_2 \log(u) + \text{perms}(u, v, w), \quad (\text{B.4})$$

$$\mathcal{R}_{\hat{\mathcal{O}}_1, \alpha; 2}^{(2), N_c^2} = \left(\frac{u^2}{w^2} - \frac{1}{2} \right) T_2(u, v) - \frac{55}{48} \log^2(u) - \frac{73}{72} \log(u) \log(v) + \frac{23}{6} \zeta_2 + \text{perms}(u, v, w), \quad (\text{B.5})$$

$$\mathcal{R}_{\hat{\mathcal{O}}_1, \alpha; 1}^{(2), N_c^2} = \left(\frac{119}{18} + \frac{v}{w} + \frac{u^2}{2vw} \right) \log(u) + \text{perms}(u, v, w), \quad (\text{B.6})$$

$$\mathcal{R}_{\hat{\mathcal{O}}_1, \alpha; 0}^{(2), N_c^2} = \frac{487}{72} \frac{1}{uvw} - \frac{14075}{216}, \quad (\text{B.7})$$

and $R_{\text{L3;4}}^{(2)}(u, v, w)$, $T_3(u, v, w)$, $T_2(u, v)$ are defined in (6.2), (6.4) and (6.5) respectively.

In (B.5), there seems to be $\frac{1}{w^2}$ -type unphysical poles. Such poles can be cancelled by the zero of $T_2(u, v)$ when $w \rightarrow 0$:

$$T(u, 1 - u - w) = -w \left[\frac{\ln u}{1 - u} + \frac{\ln(1 - u)}{u} \right] + \mathcal{O}(w^2). \quad (\text{B.8})$$

The n_f parts are simpler and we collect terms of different degrees together:

$$\mathcal{R}_{\hat{\mathcal{O}}_1, \alpha}^{(2), N_c n_f} = \frac{1}{12} \zeta_2 \log(u) - \frac{13\zeta_3}{36} - \frac{\log^2(u)}{4} + \frac{1}{18} \log(u) \log(v) - \frac{95\zeta_2}{72} - \frac{64 \log(u)}{27} + \frac{2863}{648} + \text{perms}(u, v, w), \quad (\text{B.9})$$

$$\mathcal{R}_{\hat{\mathcal{O}}_1, \alpha}^{(2), n_f^2} = \frac{\log^2(u)}{12} + \frac{1}{18} \log(u) \log(v) + \frac{\zeta_2}{36} - \frac{5 \log(u)}{27} + \text{perms}(u, v, w). \quad (\text{B.10})$$

Finally, the terms containing $\log(-q^2)$ are give by:

$$\begin{aligned} \mathcal{R}_{\hat{\mathcal{O}}_1, \alpha; \log(-q^2)}^{(2)} &= \left(-\frac{19}{24} N_c^2 - \frac{7N_c n_f}{6} + \frac{5n_f^2}{6} \right) \log^2(-q^2) \\ &+ \left[N_c^2 \left(-3\zeta_3 - \frac{11\zeta_2}{4} - \frac{19}{36} \log(uvw) - \frac{2}{uvw} + \frac{119}{3} \right) \right. \\ &\quad \left. + N_c n_f \left(\frac{\zeta_2}{2} - \frac{7}{9} \log(uvw) - \frac{128}{9} \right) + n_f^2 \left(\frac{5}{9} \log(uvw) - \frac{10}{9} \right) \right] \log(-q^2). \end{aligned} \quad (\text{B.11})$$

B.2 $\hat{\mathcal{O}}_1 \rightarrow (1^-, 2^-, 3^+)$

The $(1^-, 2^-, 3^+)$ configuration is very simple:

$$\begin{aligned} r_{\hat{\mathcal{O}}_1, \beta}^{(2), \text{fin}} &= N_c^2 \left\{ \left[T_2(u, v) + u \log(u) + \text{cyclic perms}(u, v, w) \right] + \frac{487}{72} - \frac{vw}{36u} \right\} \\ &+ N_c n_f \frac{vw}{18u} - 2N_c^2 \log(-q^2). \end{aligned} \quad (\text{B.12})$$

B.3 $\hat{\mathcal{O}}_1 \rightarrow (1^q, 2^{\bar{q}}, 3^-)$

We decompose the two-loop finite remainder according to the color factors as:

$$r_{\hat{\mathcal{O}}_1, \gamma}^{(2), \text{fin}} = N_c^2 \mathcal{R}_{\hat{\mathcal{O}}_1, \gamma}^{(2), N_c^2} + N_c^0 \mathcal{R}_{\hat{\mathcal{O}}_1, \gamma}^{(2), N_c^0} + N_c n_f \mathcal{R}_{\hat{\mathcal{O}}_1, \gamma}^{(2), N_c n_f} + \mathcal{R}_{\hat{\mathcal{O}}_1, \gamma; \log(-q^2)}^{(2)}, \quad (\text{B.13})$$

where

$$\begin{aligned} \mathcal{R}_{\hat{\mathcal{O}}_1, \gamma}^{(2), N_c^2} &= \frac{uv}{w} T_2(u, v) + \frac{uw}{v} T_2(u, w) + u \left(\frac{19 \log(u)}{18} + \frac{\log(v)}{18} - \frac{\log(w)}{72} \right) \\ &+ \frac{u^2}{72v} + \frac{u}{72v} - \frac{1501u}{432} + \frac{487}{72}, \end{aligned} \quad (\text{B.14})$$

$$\mathcal{R}_{\hat{\mathcal{O}}_1, \gamma}^{(2), N_c^0} = -\frac{vw}{u} T_2(v, w) + \frac{u(-1885v + 6w + 6)}{432v} + \left(\frac{u}{12} - v \right) \log(v) + \left(\frac{u}{36} - w \right) \log(w), \quad (\text{B.15})$$

$$\mathcal{R}_{\hat{\mathcal{O}}_1, \gamma}^{(2), N_c n_f} = \frac{1}{9} u \left(-\log(u) - \frac{\log(v)}{8} - \frac{\log(w)}{8} + \frac{31}{12} \right), \quad (\text{B.16})$$

$$\mathcal{R}_{\hat{\mathcal{O}}_1, \gamma; \log(-q^2)}^{(2)} = \left[-\frac{5}{36} u N_c n_f + \left(\frac{79u}{72} - 2 \right) N_c^2 + \frac{10u}{9} \right] \log(-q^2), \quad (\text{B.17})$$

and $T_2(u, v)$ are defined in (6.5).

C Two-loop remainder of $F_{\hat{\mathcal{O}}_3}$

For $\hat{\mathcal{O}}_3$ with three partons, only the $(1^q, 2^{\bar{q}}, 3^-)$ -configuration is non-zero. We have

$$\begin{aligned} r_{\hat{\mathcal{O}}_3, \gamma}^{(2), \text{fin}} &= N_c n_f \left(\frac{5 \log(v)}{36} - \frac{251}{432} \right) + \frac{n_f}{N_c} \left(\frac{\log(v)}{9} - \frac{43}{108} \right) + \frac{1}{N_c^2} \left(\frac{7 \log(v)}{36} - \frac{331}{432} \right) \\ &+ \left(\frac{\log(v)}{18} - \frac{23}{108} \right) + \log(-q^2) \left(\frac{5N_c n_f}{36} + \frac{n_f}{9N_c} + \frac{7}{36N_c^2} + \frac{1}{18} \right). \end{aligned} \quad (\text{C.1})$$

D Two-loop remainder of $F_{\hat{O}_4}$

D.1 $\hat{O}_4 \rightarrow (1^-, 2^-, 3^-)$

We decompose the two-loop finite remainder according to the color factors as:

$$r_{\hat{O}_4, \alpha}^{(2), \text{fin}} = N_c n_f \mathcal{R}_{\hat{O}_4, \alpha}^{(2), N_c n_f} + \frac{n_f}{N_c} \mathcal{R}_{\hat{O}_4, \alpha}^{(2), n_f / N_c} + n_f^2 \mathcal{R}_{\hat{O}_4, \alpha}^{(2), n_f^2} + \mathcal{R}_{\hat{O}_4, \alpha; \log(-q^2)}^{(2)}, \quad (\text{D.1})$$

where

$$\begin{aligned} \mathcal{R}_{\hat{O}_4, \alpha}^{(2), N_c n_f} &= \left(\frac{2u^3 v^3}{w^3} + \frac{5u^2 v^2}{2w^2} + \frac{uv}{w} \right) T_2(u, v) \\ &+ \left(\frac{4u^3 v^2}{w^2} + \frac{3u^3 v}{w} + \frac{5u^2 v^2}{w} + \frac{5u^3}{12} + \frac{13u^2 v}{2} + 2uv^2 + \frac{109uvw}{36} \right) \log(u) \\ &+ \left(\frac{221u^3}{72} + \frac{81u^2 v}{4} + \frac{655uvw}{108} + \frac{u^2 v^2}{w} \right), \end{aligned} \quad (\text{D.2})$$

$$\begin{aligned} \mathcal{R}_{\hat{O}_4, \alpha}^{(2), n_f / N_c} &= -\frac{u^3 v^3}{3w^3} T_2(u, v) + \left(-\frac{2u^3 v^2}{3w^2} + \frac{u^3 v}{3w} - \frac{u^3}{9} + \frac{uvw}{6} \right) \log(u) \\ &+ \left(-\frac{139}{216} u^3 - \frac{15u^2 v}{4} - \frac{55uvw}{27} - \frac{u^2 v^2}{6w} \right), \end{aligned} \quad (\text{D.3})$$

$$\mathcal{R}_{\hat{O}_4, \alpha}^{(2), n_f^2} = -\frac{5}{18} uvw \log(u) + \frac{5uvw}{27}, \quad (\text{D.4})$$

$$\mathcal{R}_{\hat{O}_4, \alpha; \log(-q^2)}^{(2)} = \left\{ \left(\frac{4}{9N_c} - \frac{5N_c}{3} \right) n_f + \left[\left(\frac{4}{3N_c} + \frac{25N_c}{6} \right) n_f - \frac{5n_f^2}{3} \right] uvw \right\} \log(-q^2), \quad (\text{D.5})$$

and $T_2(u, v)$ are defined in (6.5).

D.2 $\hat{O}_4 \rightarrow (1^-, 2^-, 3^+)$

We decompose the two-loop finite remainder according to the color factors as:

$$r_{\hat{O}_4, \beta}^{(2), \text{fin}} = N_c n_f \mathcal{R}_{\hat{O}_4, \beta}^{(2), N_c n_f} + \frac{n_f}{N_c} \mathcal{R}_{\hat{O}_4, \beta}^{(2), n_f / N_c} + n_f^2 \mathcal{R}_{\hat{O}_4, \beta}^{(2), n_f^2} + \mathcal{R}_{\hat{O}_4, \beta; \log(-q^2)}^{(2)}, \quad (\text{D.6})$$

where

$$\begin{aligned}
\mathcal{R}_{\hat{O}_{4,\beta}}^{(2),N_c n_f} &= \frac{2}{3} v T_3(v, u, w) - \left(\frac{2v^3 w}{3u^3} + \frac{v^2 w}{u^2} + \frac{vw}{u} \right) T_3(w, v, u) \\
&+ vw \left(\frac{4v^2 w^2}{u^5} + \frac{5vw}{4u^4} - \frac{35vw}{12u^3} + \frac{11}{12u^3} - \frac{1}{4u^2} + \frac{7}{6u} \right) T_2(v, w) \\
&+ \left(\frac{4uv^3}{w^3} + \frac{v}{3uw} - \frac{25v^3}{6w^2} + \frac{5v^2}{w^2} - \frac{13v^2}{2w} + \frac{5v}{3w} - \frac{7v}{3} \right) T_2(u, v) \\
&+ \frac{2(1-v)vw}{3u^2} \left(\text{Li}_2(1-v) + \frac{\log^2(v)}{2} \right) \\
&+ \left(\frac{4uv^2}{w^2} + \frac{5vw}{6u} + \frac{15u}{8} + \frac{1}{6u} - \frac{13v^2}{6w} + \frac{3v}{w} - \frac{13}{8} \right) \log(u) \\
&+ \left(\frac{8v^3 w^2}{u^4} + \frac{4v^2 w^2}{u^3} - \frac{3v^2 w}{2u^3} + \frac{19v^3}{6u^2} - \frac{7v^2}{4u^2} + \frac{7v}{6u^2} + \frac{37u^2}{6w} + \frac{44w^2}{9u} \right. \\
&\quad \left. - \frac{383w}{36u} - \frac{27u}{2w} - \frac{7}{6uw} + \frac{47u}{4} + \frac{83}{12u} + \frac{4v^3}{w^2} + \frac{5}{3(v-1)} - \frac{4}{3(v-1)^2} \right. \\
&\quad \left. + \frac{377w}{36} + \frac{17}{2w} - \frac{47}{3} \right) \log(v) \\
&+ \left(\frac{2v^2 w^2}{u^3} - \frac{vw}{24u^2} - \frac{385vw}{216u} - \frac{25u}{24} + \frac{13}{24u} + \frac{2v^2}{w} + \frac{4}{3(v-1)} + \frac{353}{72} \right) + (v \leftrightarrow w),
\end{aligned} \tag{D.7}$$

$$\begin{aligned}
\mathcal{R}_{\hat{O}_{4,\beta}}^{(2),n_f/N_c} &= \left(\frac{2v^4}{3w^3} - \frac{2v^3}{3w^3} + \frac{2v^3}{9w^2} + \frac{4v}{9} \right) T_2(u, v) \\
&- vw \left(\frac{2v^2 w^2}{3u^5} + \frac{2vw}{3u^4} - \frac{4vw}{9u^3} + \frac{2}{9u^3} - \frac{1}{9u^2} + \frac{2}{9u} \right) T_2(v, w) \\
&+ \left(-\frac{u}{18} + \frac{2w^3}{3v^2} - \frac{2w^2}{3v^2} - \frac{v^2}{9w} + \frac{v}{3w} - \frac{1}{18} \right) \log(u) \\
&- \left(\frac{4v^3 w^2}{3u^4} + \frac{2(v^2 w^2 + v^2 w)}{3u^3} + \frac{2(3vw^2 - 2vw + v)}{9u^2} + \frac{vw}{9u} + \frac{v}{9uw} + \frac{2v}{9u} \right. \\
&\quad \left. + \frac{2v^3}{3w^2} - \frac{v^2}{9w} - \frac{v}{9w} + \frac{v}{9} + \frac{2}{9(v-1)} - \frac{2}{9(v-1)^2} + \frac{4}{9} \right) \log(v) \\
&- \left(\frac{v^2 w^2}{3u^3} + \frac{2vw}{9u^2} + \frac{19vw}{36u} + \frac{u}{9} + \frac{1}{6u} + \frac{w^2}{3v} + \frac{2}{9(v-1)} + \frac{127}{216} \right) + (v \leftrightarrow w),
\end{aligned} \tag{D.8}$$

$$\mathcal{R}_{\hat{O}_{4,\beta}}^{(2),n_f^2} = \frac{10vw}{27u} - \frac{vw(3 \log(u) + \log(v) + \log(w))}{9u}, \tag{D.9}$$

$$\mathcal{R}_{\hat{O}_{4,\beta}; \log(-q^2)}^{(2)} = \left(-\frac{5N_c n_f (6u - 5vw)}{18u} + \frac{4n_f (u + vw)}{9u N_c} - \frac{5vwn_f^2}{9u} \right) \log(-q^2), \tag{D.10}$$

and $T_3(u, v, w)$ and $T_2(u, v)$ are defined in (6.4) and (6.5) respectively.

D.3 $\hat{O}_4 \rightarrow (1^q, 2\bar{q}, 3^-)$

The two-loop finite remainder can be decomposed according to the color factors as:

$$\begin{aligned} r_{\hat{O}_4, \gamma}^{(2), \text{fin}} = & N_c^2 \mathcal{R}_{\hat{O}_4, \gamma}^{(2), N_c^2} + N_c^0 \mathcal{R}_{\hat{O}_4, \gamma}^{(2), N_c^0} + \frac{1}{N_c^2} \mathcal{R}_{\hat{O}_4, \gamma}^{(2), N_c^{-2}} + \frac{n_f}{N_c} \mathcal{R}_{\hat{O}_4, \gamma}^{(2), n_f/N_c} + N_c n_f \mathcal{R}_{\hat{O}_4, \gamma}^{(2), N_c n_f} \\ & + n_f^2 \mathcal{R}_{\hat{O}_4, \gamma}^{(2), n_f^2} + \mathcal{R}_{\hat{O}_4, \gamma; \log(-q^2)}^{(2)}. \end{aligned} \quad (\text{D.11})$$

We further decompose the functions according to transcendentality degree d as

$$\mathcal{R}_{\hat{O}_4, \gamma}^{(2)} = \sum_{d=0}^4 \mathcal{R}_{\hat{O}_4, \gamma; d}^{(2)}. \quad (\text{D.12})$$

The degree-4 part:

$$\begin{aligned} \mathcal{R}_{\hat{O}_4; \gamma; 4}^{(2), N_c^2} = & G(1-v, 1-v, 1, 0, w) - \text{Li}_4(1-v) - \text{Li}_4(v) + \text{Li}_4\left(\frac{v-1}{v}\right) + \text{Li}_3(v) \log\left(\frac{u}{1-v}\right) \\ & + \text{Li}_3\left(\frac{u}{1-v}\right) \log(v) + [\text{Li}_3(v) + \text{Li}_3(1-v)] \left[\log(w) - 2 \log\left(\frac{u}{1-v}\right) \right] \\ & + \text{Li}_2\left(\frac{u}{1-v}\right) \text{Li}_2\left(\frac{v-1}{v}\right) + \frac{1}{2} \text{Li}_2(v) \log^2\left(\frac{u}{1-v}\right) + \text{Li}_2(1-v) \log(1-v) \log\left(\frac{u}{1-v}\right) \\ & + \frac{1}{24} \log^2(v) \left[\log(v) \log\left(\frac{v}{(1-v)^4}\right) - 3 \log(w) \log\left(\frac{w}{(1-v)^4}\right) \right] \\ & + \zeta_2 \left[\text{Li}_2(1-v) + \log(v) \log\left(\frac{v}{w}\right) - \frac{1}{2} \log^2\left(\frac{u}{1-v}\right) \right] + \zeta_3 \left[\log\left(\frac{u}{1-v}\right) - 5 \log(v) \right] \\ & + \frac{23\zeta_4}{8} + \{v \leftrightarrow w\}, \end{aligned}$$

$$\mathcal{R}_{\hat{O}_4; \gamma; 4}^{(2), 1/N_c^2} = 6\zeta_3 \log(u) - \frac{11}{2} \zeta_4,$$

$$\mathcal{R}_{\hat{O}_4; \gamma; 4}^{(2), N_c^0} = - \left(R_{\text{L3;4}}^{(2)} - \mathcal{R}_{\hat{O}_4; \gamma; 4}^{(2), 1/N_c^2} - \mathcal{R}_{\hat{O}_4; \gamma; 4}^{(2), N_c^2} \right). \quad (\text{D.13})$$

The n_f parts do not contribute to the maximal transcendentality part.

The degree-3 part:

$$\mathcal{R}_{\hat{O}_4; \gamma; 3}^{(2), N_c^2} = \left(1 + \frac{w}{u}\right) T_3(v, w, u) + \frac{1}{3} \left(1 + \frac{v}{u}\right) T_3(w, v, u) + \zeta_2 \left[\frac{7 \log(v)}{4} + \frac{\log(w)}{12} \right] + \frac{257\zeta_3}{18}, \quad (\text{D.14})$$

$$\begin{aligned} \mathcal{R}_{\hat{O}_4; \gamma; 3}^{(2), N_c^0} = & - \left[\frac{1}{2} \left(\frac{w}{v} + 1\right)^2 + \frac{w}{v} + 1 \right] T_3(u, w, v) + T_3(v, u, w) - T_3(v, w, u) \\ & + \left[\frac{1}{6} \left(\frac{u}{v} + 1\right)^2 - \frac{4}{3} \left(\frac{u}{v} + 1\right) + \frac{1}{3} \right] T_3(w, u, v) - \frac{1}{3} T_3(w, v, u) \\ & - \zeta_2 \left[\frac{31 \log(u)}{12} - \frac{5 \log(v)}{3} - \frac{7 \log(w)}{6} \right] - \frac{137\zeta_3}{36}, \end{aligned} \quad (\text{D.15})$$

$$\begin{aligned} \mathcal{R}_{\hat{O}_4; \gamma; 3}^{(2), N_c^{-2}} = & \frac{w}{u} T_3(v, w, u) + \frac{1}{3} \frac{v}{u} T_3(w, v, u) + T_3(v, u, w) + \frac{1}{3} T_3(w, u, v) \\ & - \frac{\zeta_2}{3} (5 \log(u) + 3 \log(v) + \log(w)) - \frac{15\zeta_3}{2}, \end{aligned} \quad (\text{D.16})$$

$$\mathcal{R}_{\hat{\mathcal{O}}_4; \gamma; 3}^{(2), N_c n_f} = \frac{2}{3} T_3(u, v, w) + \frac{2}{3} T_3(u, w, v) - \frac{\zeta_2}{6} (8 \log(u) - 3 \log(v) - 3 \log(w)) - \frac{43\zeta(3)}{9}, \quad (\text{D.17})$$

$$\mathcal{R}_{\hat{\mathcal{O}}_4; \gamma; 3}^{(2), n_f / N_c} = \frac{\zeta_2}{2} \log(u) - \frac{71\zeta_3}{18}, \quad (\text{D.18})$$

$$\mathcal{R}_{\hat{\mathcal{O}}_4; \gamma; 3}^{(2), n_f^2} = 0, \quad (\text{D.19})$$

and $T_3(u, v, w)$ are defined in (6.4).

The degree-2 part:

$$\begin{aligned} \mathcal{R}_{\hat{\mathcal{O}}_4; \gamma; 2}^{(2), N_c^2} &= \left(-\frac{v(1-v)^2}{6u^3} + \frac{(3v+5)(1-v)}{12u^2} + \frac{-8v^2-15v+6}{18uv} \right) T_2(v, w) \\ &\quad - \frac{13\text{Li}_2(1-w)}{36} + \frac{8}{9} \log(v) \log(w) + \frac{17 \log^2(v)}{18} - \frac{35 \log^2(w)}{36} + \frac{25\pi^2}{18}, \end{aligned} \quad (\text{D.20})$$

$$\begin{aligned} \mathcal{R}_{\hat{\mathcal{O}}_4; \gamma; 2}^{(2), N_c^0} &= - \left(-\frac{(1-u)^2 u^2}{2v^4} + \frac{(1-u)(5u+2)u}{6v^3} - \frac{7-3u}{6v^2} - \frac{8-3u}{6v} + \frac{9}{4} \right) T_2(u, w) \\ &\quad - \left(-\frac{2v(1-v)^2}{3u^3} + \frac{(v+1)(1-v)}{3u^2} - \frac{39-29v}{18u} + \frac{u}{6v} - \frac{6-23v}{18v} \right) T_2(v, w) \\ &\quad + \left(-\frac{5v^2+v-1}{6vw} - \frac{v(1-v)^2}{3w^3} + \frac{(9v+1)(1-v)}{12w^2} - \frac{w}{6v} - \frac{5v+1}{6v} \right) T_2(u, v) \\ &\quad + \left(\frac{7}{4} - \frac{u}{6v} \right) \left(\text{Li}_2(1-w) + \frac{\log^2(w)}{2} \right) + \frac{(-u+5v+1)}{2v} \left(\text{Li}_2(1-u) + \frac{\log^2(u)}{2} \right) \\ &\quad + \frac{35\text{Li}_2(1-v)}{18} + \frac{7 \log^2(v)}{2} + \frac{7 \log^2(w)}{12} - \frac{137\pi^2}{108}, \end{aligned} \quad (\text{D.21})$$

$$\begin{aligned} \mathcal{R}_{\hat{\mathcal{O}}_4; \gamma; 2}^{(2), N_c^{-2}} &= - \left(\frac{7(1-u)^2 u^2}{3v^4} + \frac{101u^2 - 57u + 3}{18v^2} + \frac{(3-20u)(1-u)u}{3v^3} - \frac{2-7u}{3v} + 1 \right) T_2(u, w) \\ &\quad + \left(\frac{14(1-u)u^2}{9w^3} + \frac{u+6v-2}{6v} + \frac{(24-61u)u}{18w^2} + \frac{2-17u}{6w} \right) T_2(u, v) \\ &\quad + \left(-\frac{v(1-v)^2}{u^3} + \frac{(1-v)^2}{3u^2} - \frac{v^2-6v+3}{18uv} - \frac{u}{6v} + \frac{1-2v}{3v} \right) T_2(v, w) \\ &\quad - \frac{4\text{Li}_2(1-v)}{3} - \frac{17\text{Li}_2(1-w)}{18} - \frac{1}{4} \log^2(w) + \frac{31\pi^2}{24}, \end{aligned} \quad (\text{D.22})$$

$$\begin{aligned} \mathcal{R}_{\hat{\mathcal{O}}_4; \gamma; 2}^{(2), N_c n_f} &= - \left(\frac{11(1-u)^2 u^2}{6v^4} + \frac{131u^2 - 90u + 6}{18v^2} + \frac{(5-18u)(1-u)u}{3v^3} - \frac{5(1-3u)}{3v} + \frac{16}{9} \right) T_2(u, w) \\ &\quad + \left(\frac{11v(1-v)^2}{9w^3} - \frac{(v+3)(1-v)}{9w^2} + \frac{2v}{9w} - \frac{4}{9} \right) T_2(u, v) - \frac{1}{12} T_2(v, w) - \frac{10}{9} \text{Li}_2(1-u) \\ &\quad + \frac{19}{36} \text{Li}_2(1-v) - \frac{\text{Li}_2(1-w)}{36} - \frac{35}{18} \log^2(u) - \frac{23}{36} \log^2(v) - \frac{2}{9} \log^2(w) - \frac{11\pi^2}{27}, \end{aligned} \quad (\text{D.23})$$

$$\begin{aligned} \mathcal{R}_{\hat{O}_4; \gamma; 2}^{(2), n_f / N_c} &= \left(\frac{2(2w+1)}{9u} - \frac{4}{9} \right) T_2(v, w) + \frac{8\text{Li}_2(1-u)}{9} + \frac{8\text{Li}_2(1-v)}{9} + \frac{4\text{Li}_2(1-w)}{9} \\ &\quad - \frac{1}{2} \log^2(v) - \frac{\log^2(w)}{6} - \frac{25\pi^2}{108}, \end{aligned} \quad (\text{D.24})$$

$$\begin{aligned} \mathcal{R}_{\hat{O}_4; \gamma; 2}^{(2), n_f^2} &= \frac{1}{9} \log(u) \log(v) + \frac{1}{9} \log(u) \log(w) + \frac{4\log^2(u)}{9} + \frac{1}{36} \log(v) \log(w) + \frac{5\log^2(v)}{72} \\ &\quad + \frac{5\log^2(w)}{72} + \frac{\pi^2}{108}, \end{aligned} \quad (\text{D.25})$$

and $T_2(u, v)$ are defined in (6.5).

The degree-1 part:

$$\begin{aligned} \mathcal{R}_{\hat{O}_4; \gamma; 1}^{(2), N_c^2} &= \left(\frac{v^2}{6u^2} - \frac{v}{6u^2} + \frac{v}{6u} + \frac{13u}{18v} + \frac{5}{12u} + \frac{19}{18v} + \frac{101}{12} \right) \log(v) \\ &\quad + \left(-\frac{w^2}{6u^2} - \frac{w^2}{6uv} + \frac{2w}{3uv} - \frac{u}{6v} - \frac{w}{3u} - \frac{11w}{36v} - \frac{2}{9v(1-w)} + \frac{5}{18v} + \frac{391}{24} \right) \log(w), \end{aligned} \quad (\text{D.26})$$

$$\begin{aligned} \mathcal{R}_{\hat{O}_4; \gamma; 1}^{(2), N_c^0} &= \left(\frac{u^2w}{2v^3} - \frac{5u^2}{12v^2} + \frac{u^2}{4vw} - \frac{u^2}{3w^2} - \frac{uw}{3v^2} + \frac{3u}{4v} + \frac{u}{6w} + \frac{w}{4v} - \frac{2651}{216} \right) \log(u) \\ &\quad + \left(\frac{u^2}{3w^2} - \frac{2w^2}{3u^2} + \frac{2w}{3u^2} - \frac{u}{3w^2} + \frac{u}{12w} - \frac{4w}{3u} + \frac{1}{3u} + \frac{29w}{36v} + \frac{8}{9v} + \frac{1}{3w} - \frac{247}{27} \right) \log(v) \\ &\quad + \left(\frac{2w^2}{3u^2} + \frac{11uw^2}{12v^3} + \frac{uw}{12v^2} - \frac{2w}{3uv} + \frac{4w}{3u} + \frac{5w^3}{12v^3} - \frac{5w^2}{12v^3} + \frac{w^2}{12v^2} - \frac{w}{4v^2} \right. \\ &\quad \left. + \frac{13}{9v(1-w)} - \frac{4}{3v} + \frac{733}{216} \right) \log(w), \end{aligned} \quad (\text{D.27})$$

$$\begin{aligned} \mathcal{R}_{\hat{O}_4; \gamma; 1}^{(2), N_c^{-2}} &= \left(-\frac{7u^2w}{3v^3} + \frac{13u^2}{6v^2} - \frac{23u^2}{18vw} + \frac{14u^2}{9w^2} - \frac{uw}{v^2} - \frac{u}{12v} + \frac{4u}{3w} - \frac{w}{2v} - \frac{5}{8} \right) \log(u) \\ &\quad + \left(-\frac{14u^2}{9w^2} + \frac{w^2}{u^2} - \frac{w}{u^2} + \frac{14u}{9w^2} - \frac{47u}{18w} + \frac{17w}{6u} - \frac{3}{2u} - \frac{w}{12v} - \frac{1}{12v} + \frac{5}{9w} - \frac{40}{9} \right) \log(v) \\ &\quad + \left(-\frac{w^2}{u^2} - \frac{3uw^2}{2v^3} + \frac{uw}{v^2} + \frac{5w^2}{6uv} + \frac{5u}{6v} - \frac{2w}{u} + \frac{5w^3}{6v^3} - \frac{5w^2}{6v^3} + \frac{w^2}{v^2} + \frac{5w}{3v} \right. \\ &\quad \left. - \frac{11}{9v(1-w)} + \frac{10}{9v} - \frac{73}{36} \right) \log(w), \end{aligned} \quad (\text{D.28})$$

$$\begin{aligned} \mathcal{R}_{\hat{O}_4; \gamma; 1}^{(2), N_c n_f} &= \left(\frac{11u^3}{6v^3} - \frac{11u^2}{6v^3} + \frac{61u^2}{12v^2} - \frac{5u}{3v^2} + \frac{43u}{9v} - \frac{3}{1-u} - \frac{4}{3(1-u)^2} + \frac{11v^2}{9w^2} - \frac{22v}{9w^2} - \frac{v}{2w} \right. \\ &\quad \left. - \frac{17}{18vw} + \frac{11}{18v} + \frac{11}{9w^2} + \frac{13}{9w} + \frac{154}{27} \right) \log(u) \\ &\quad + \left(-\frac{11v^2}{9w^2} + \frac{11v}{9w^2} + \frac{v}{2w} + \frac{5w}{36v} - \frac{5}{18v} - \frac{1}{3w} + \frac{7}{108} \right) \log(v) \\ &\quad + \left(\frac{11w^3}{6v^3} - \frac{11w^2}{6v^3} + \frac{5w^2}{12v^2} + \frac{2w}{3v^2} - \frac{9w^2 - 11w + 6}{36v(1-w)} - \frac{223}{54} \right) \log(w), \end{aligned} \quad (\text{D.29})$$

$$\begin{aligned}\mathcal{R}_{\hat{O}_{4;\gamma;1}}^{(2),n_f/N_c} &= \left(\frac{4}{9(1-u)} + \frac{2}{9(1-u)^2} + \frac{269}{54} \right) \log(u) - \left(\frac{1-5w^2}{36v(1-w)} - \frac{119}{54} \right) \log(w) \\ &\quad + \left(-\frac{5w}{36v} - \frac{5}{36v} + \frac{275}{54} \right) \log(v),\end{aligned}\tag{D.30}$$

$$\mathcal{R}_{\hat{O}_{4;\gamma;1}}^{(2),n_f^2} = -\frac{40 \log(u)}{27} - \frac{10 \log(v)}{27} - \frac{10 \log(w)}{27}.\tag{D.31}$$

The degree-0 part:

$$\mathcal{R}_{\hat{O}_{4;\gamma;0}}^{(2),N_c^2} = -\frac{w}{12u} + \frac{143w}{72v} - \frac{3}{v} - \frac{44245}{864},\tag{D.32}$$

$$\mathcal{R}_{\hat{O}_{4;\gamma;0}}^{(2),N_c^0} = -\frac{v}{3u} + \frac{1}{3u} - \frac{w^2}{4v^2} + \frac{w}{4v^2} - \frac{25w}{36v} + \frac{v}{6w} - \frac{301}{72v} - \frac{1}{6w} + \frac{5851}{324},\tag{D.33}$$

$$\mathcal{R}_{\hat{O}_{4;\gamma;0}}^{(2),N_c^{-2}} = \frac{13uw}{24v^2} - \frac{w}{2u} + \frac{7u}{9w} + \frac{41w^2}{24v^2} - \frac{41w}{24v^2} - \frac{9}{8v} + \frac{32303}{2592},\tag{D.34}$$

$$\mathcal{R}_{\hat{O}_{4;\gamma;0}}^{(2),N_c n_f} = -\frac{4}{3(1-u)} + \frac{221}{36u} + \frac{11w^2}{12v^2} - \frac{11w}{12v^2} - \frac{4w}{3v} - \frac{11v}{18w} + \frac{85}{36v} + \frac{11}{18w} + \frac{4435}{648},\tag{D.35}$$

$$\mathcal{R}_{\hat{O}_{4;\gamma;0}}^{(2),n_f/N_c} = -\frac{2u}{3v} + \frac{2}{9(1-u)} - \frac{139}{108u} + \frac{4}{3v} - \frac{11273}{648},\tag{D.36}$$

$$\mathcal{R}_{\hat{O}_{4;\gamma;0}}^{(2),n_f^2} = \frac{100}{81}.\tag{D.37}$$

Finally, the terms containing $\log(-q^2)$ are give by:

$$\begin{aligned}\mathcal{R}_{\hat{O}_{4;\gamma;\log(-q^2)}}^{(2)} &= \left[N_c^2 \left(-\frac{25w}{36v} + \frac{25}{18v} + \frac{25 \log(v)}{9} - \frac{25 \log(w)}{36} - 8\zeta(3) + \frac{11\zeta_2}{6} + \frac{1739}{72} \right) \right. \\ &\quad + \frac{1}{N_c^2} \left(\frac{2w}{9v} + \frac{2}{9v} + \frac{4 \log(v)}{3} + \frac{4 \log(w)}{9} + 6\zeta(3) - 3\zeta_2 - \frac{167}{24} \right) \\ &\quad + N_c n_f \left(-\frac{5}{3u} - \frac{25 \log(u)}{9} + \frac{5w}{18v} - \frac{5}{9v} - \frac{65 \log(v)}{36} - \frac{5 \log(w)}{12} - \frac{\zeta_2}{3} + \frac{1}{9} \right) \\ &\quad + \frac{n_f}{N_c} \left(\frac{4}{9u} - \frac{8 \log(u)}{9} - \frac{5w}{18v} - \frac{5}{18v} - \frac{17 \log(v)}{9} - \frac{7 \log(w)}{9} + \frac{\zeta_2}{2} + \frac{221}{18} \right) \\ &\quad + n_f^2 \left(\frac{10 \log(u)}{9} + \frac{5 \log(v)}{18} + \frac{5 \log(w)}{18} - \frac{20}{9} \right) \\ &\quad + \left. \left(\zeta(3) + \frac{\zeta_2}{4} + \frac{17w}{36v} + \frac{41}{36v} + \frac{91 \log(v)}{18} + \frac{7 \log(w)}{6} - \frac{341}{18} \right) \right] \log(-q^2) \\ &\quad + \left(-\frac{5N_c n_f}{2} - \frac{16n_f}{9N_c} + \frac{25N_c^2}{24} + \frac{8}{9N_c^2} + \frac{5n_f^2}{6} + \frac{28}{9} \right) \log^2(-q^2).\end{aligned}\tag{D.38}$$

References

- [1] **ATLAS** Collaboration, G. Aad et al., *Observation of a new particle in the search for the Standard Model Higgs boson with the ATLAS detector at the LHC*, *Phys. Lett.* **B716** (2012) 1–29, [[arXiv:1207.7214](https://arxiv.org/abs/1207.7214)].

- [2] **CMS Collaboration**, S. Chatrchyan et al., *Observation of a New Boson at a Mass of 125 GeV with the CMS Experiment at the LHC*, *Phys. Lett.* **B716** (2012) 30–61, [[arXiv:1207.7235](#)].
- [3] **CEPC Study Group Collaboration**, *CEPC Conceptual Design Report: Volume 1 - Accelerator*, [arXiv:1809.00285](#).
- [4] **CEPC Study Group Collaboration**, M. Dong et al., *CEPC Conceptual Design Report: Volume 2 - Physics & Detector*, [arXiv:1811.10545](#).
- [5] **FCC Collaboration**, A. Abada et al., *FCC Physics Opportunities*, *Eur. Phys. J.* **C79** (2019), no. 6 474.
- [6] **FCC Collaboration**, A. Abada et al., *FCC-ee: The Lepton Collider*, *Eur. Phys. J. ST* **228** (2019), no. 2 261–623.
- [7] **FCC Collaboration**, A. Abada et al., *FCC-hh: The Hadron Collider*, *Eur. Phys. J. ST* **228** (2019), no. 4 755–1107.
- [8] Z. Xu, D.-H. Zhang, and L. Chang, *Helicity Amplitudes for Multiple Bremsstrahlung in Massless Nonabelian Gauge Theories*, *Nucl. Phys.* **B291** (1987) 392–428.
- [9] P. De Causmaecker, R. Gastmans, W. Troost, and T. T. Wu, *Multiple Bremsstrahlung in Gauge Theories at High-Energies. 1. General Formalism for Quantum Electrodynamics*, *Nucl. Phys.* **B206** (1982) 53–60.
- [10] F. A. Berends, R. Kleiss, P. De Causmaecker, R. Gastmans, and T. T. Wu, *Single Bremsstrahlung Processes in Gauge Theories*, *Phys. Lett.* **103B** (1981) 124–128.
- [11] R. Kleiss and W. J. Stirling, *Spinor Techniques for Calculating p anti- $p \rightarrow W^{+-} / Z0 + Jets$* , *Nucl. Phys.* **B262** (1985) 235–262.
- [12] Z. Bern, L. J. Dixon, D. C. Dunbar, and D. A. Kosower, *One loop n point gauge theory amplitudes, unitarity and collinear limits*, *Nucl.Phys.* **B425** (1994) 217–260, [[hep-ph/9403226](#)].
- [13] Z. Bern, L. J. Dixon, D. C. Dunbar, and D. A. Kosower, *Fusing gauge theory tree amplitudes into loop amplitudes*, *Nucl. Phys.* **B435** (1995) 59–101, [[hep-ph/9409265](#)].
- [14] R. Britto, F. Cachazo, and B. Feng, *Generalized unitarity and one-loop amplitudes in $N=4$ super-Yang-Mills*, *Nucl.Phys.* **B725** (2005) 275–305, [[hep-th/0412103](#)].
- [15] F. A. Berends and W. T. Giele, *Recursive Calculations for Processes with n Gluons*, *Nucl. Phys.* **B306** (1988) 759–808.
- [16] R. Britto, F. Cachazo, and B. Feng, *New recursion relations for tree amplitudes of gluons*, *Nucl. Phys.* **B715** (2005) 499–522, [[hep-th/0412308](#)].
- [17] R. Britto, F. Cachazo, B. Feng, and E. Witten, *Direct proof of tree-level recursion relation in Yang-Mills theory*, *Phys. Rev. Lett.* **94** (2005) 181602, [[hep-th/0501052](#)].
- [18] J. R. Ellis, M. K. Gaillard, and D. V. Nanopoulos, *A Phenomenological Profile of the Higgs Boson*, *Nucl. Phys.* **B106** (1976) 292.
- [19] H. M. Georgi, S. L. Glashow, M. E. Machacek, and D. V. Nanopoulos, *Higgs Bosons from Two Gluon Annihilation in Proton Proton Collisions*, *Phys. Rev. Lett.* **40** (1978) 692.
- [20] F. Wilczek, *Decays of Heavy Vector Mesons Into Higgs Particles*, *Phys. Rev. Lett.* **39** (1977) 1304.

- [21] M. A. Shifman, A. I. Vainshtein, M. B. Voloshin, and V. I. Zakharov, *Low-Energy Theorems for Higgs Boson Couplings to Photons*, *Sov. J. Nucl. Phys.* **30** (1979) 711–716. [*Yad. Fiz.*30,1368(1979)].
- [22] S. Dawson, *Radiative corrections to Higgs boson production*, *Nucl. Phys.* **B359** (1991) 283–300.
- [23] A. Djouadi, M. Spira, and P. M. Zerwas, *Production of Higgs bosons in proton colliders: QCD corrections*, *Phys. Lett.* **B264** (1991) 440–446.
- [24] B. A. Kniehl and M. Spira, *Low-energy theorems in Higgs physics*, *Z. Phys.* **C69** (1995) 77–88, [[hep-ph/9505225](#)].
- [25] K. G. Chetyrkin, B. A. Kniehl, and M. Steinhauser, *Strong coupling constant with flavor thresholds at four loops in the \overline{MS} scheme*, *Phys. Rev. Lett.* **79** (1997) 2184–2187, [[hep-ph/9706430](#)].
- [26] K. G. Chetyrkin, B. A. Kniehl, and M. Steinhauser, *Decoupling relations to $O(\alpha_s^3)$ and their connection to low-energy theorems*, *Nucl. Phys.* **B510** (1998) 61–87, [[hep-ph/9708255](#)].
- [27] T. Gehrmann, M. Jaquier, E. Glover, and A. Koukoutsakis, *Two-Loop QCD Corrections to the Helicity Amplitudes for $H \rightarrow 3$ partons*, *JHEP* **1202** (2012) 056, [[arXiv:1112.3554](#)].
- [28] R. Boughezal, F. Caola, K. Melnikov, F. Petriello, and M. Schulze, *Higgs boson production in association with a jet at next-to-next-to-leading order in perturbative QCD*, *JHEP* **06** (2013) 072, [[arXiv:1302.6216](#)].
- [29] X. Chen, T. Gehrmann, E. W. N. Glover, and M. Jaquier, *Precise QCD predictions for the production of Higgs + jet final states*, *Phys. Lett.* **B740** (2015) 147–150, [[arXiv:1408.5325](#)].
- [30] R. Boughezal, C. Focke, W. Giele, X. Liu, and F. Petriello, *Higgs boson production in association with a jet at NNLO using jetiness subtraction*, *Phys. Lett.* **B748** (2015) 5–8, [[arXiv:1505.03893](#)].
- [31] R. Boughezal, F. Caola, K. Melnikov, F. Petriello, and M. Schulze, *Higgs boson production in association with a jet at next-to-next-to-leading order*, *Phys. Rev. Lett.* **115** (2015), no. 8 082003, [[arXiv:1504.07922](#)].
- [32] R. V. Harlander, S. Liebler, and H. Mantler, *SusHi Bento: Beyond NNLO and the heavy-top limit*, *Comput. Phys. Commun.* **212** (2017) 239–257, [[arXiv:1605.03190](#)].
- [33] C. Anastasiou, C. Duhr, F. Dulat, E. Furlan, T. Gehrmann, F. Herzog, A. Lazopoulos, and B. Mistlberger, *CP-even scalar boson production via gluon fusion at the LHC*, *JHEP* **09** (2016) 037, [[arXiv:1605.05761](#)].
- [34] X. Chen, J. Cruz-Martinez, T. Gehrmann, E. W. N. Glover, and M. Jaquier, *NNLO QCD corrections to Higgs boson production at large transverse momentum*, *JHEP* **10** (2016) 066, [[arXiv:1607.08817](#)].
- [35] J. M. Lindert, K. Kudashkin, K. Melnikov, and C. Wever, *Higgs bosons with large transverse momentum at the LHC*, [[arXiv:1801.08226](#)].
- [36] S. P. Jones, M. Kerner, and G. Luisoni, *NLO QCD corrections to Higgs boson plus jet production with full top-quark mass dependence*, [[arXiv:1802.00349](#)].
- [37] T. Neumann, *NLO Higgs+jet at large transverse momenta including top quark mass effects*, [[arXiv:1802.02981](#)].

- [38] A. V. Kotikov and L. N. Lipatov, *DGLAP and BFKL equations in the $N = 4$ supersymmetric gauge theory*, *Nucl. Phys.* **B661** (2003) 19–61, [[hep-ph/0208220](#)]. [Erratum: *Nucl. Phys.* **B685**, 405(2004)].
- [39] A. Kotikov, L. Lipatov, A. Onishchenko, and V. Velizhanin, *Three loop universal anomalous dimension of the Wilson operators in $N=4$ SUSY Yang-Mills model*, *Phys.Lett.* **B595** (2004) 521–529, [[hep-th/0404092](#)].
- [40] S. Moch, J. A. M. Vermaseren, and A. Vogt, *The Three loop splitting functions in QCD: The Nonsinglet case*, *Nucl. Phys.* **B688** (2004) 101–134, [[hep-ph/0403192](#)].
- [41] T. Gehrmann and E. Remiddi, *Two loop master integrals for $\gamma^* \rightarrow 3$ jets: The Planar topologies*, *Nucl. Phys.* **B601** (2001) 248–286, [[hep-ph/0008287](#)].
- [42] T. Gehrmann and E. Remiddi, *Numerical evaluation of two-dimensional harmonic polylogarithms*, *Comput. Phys. Commun.* **144** (2002) 200–223, [[hep-ph/0111255](#)].
- [43] A. Brandhuber, G. Travaglini, and G. Yang, *Analytic two-loop form factors in $N=4$ SYM*, *JHEP* **1205** (2012) 082, [[arXiv:1201.4170](#)].
- [44] A. Brandhuber, B. Penante, G. Travaglini, and C. Wen, *The last of the simple remainders*, *JHEP* **08** (2014) 100, [[arXiv:1406.1443](#)].
- [45] F. Loebbert, D. Nandan, C. Sieg, M. Wilhelm, and G. Yang, *On-Shell Methods for the Two-Loop Dilatation Operator and Finite Remainders*, *JHEP* **10** (2015) 012, [[arXiv:1504.06323](#)].
- [46] A. Brandhuber, M. Kostacinska, B. Penante, G. Travaglini, and D. Young, *The $SU(2-3)$ dynamic two-loop form factors*, *JHEP* **08** (2016) 134, [[arXiv:1606.08682](#)].
- [47] F. Loebbert, C. Sieg, M. Wilhelm, and G. Yang, *Two-Loop $SL(2)$ Form Factors and Maximal Transcendentality*, *JHEP* **12** (2016) 090, [[arXiv:1610.06567](#)].
- [48] P. Banerjee, P. K. Dhani, M. Mahakhud, V. Ravindran, and S. Seth, *Finite remainders of the Konishi at two loops in $\mathcal{N} = 4$ SYM*, *JHEP* **05** (2017) 085, [[arXiv:1612.00885](#)].
- [49] Y. Li, A. von Manteuffel, R. M. Schabinger, and H. X. Zhu, *Soft-virtual corrections to Higgs production at N^3LO* , *Phys. Rev.* **D91** (2015) 036008, [[arXiv:1412.2771](#)].
- [50] Y. Li and H. X. Zhu, *Bootstrapping Rapidity Anomalous Dimensions for Transverse-Momentum Resummation*, *Phys. Rev. Lett.* **118** (2017), no. 2 022004, [[arXiv:1604.01404](#)].
- [51] L. J. Dixon, *The Principle of Maximal Transcendentality and the Four-Loop Collinear Anomalous Dimension*, *JHEP* **01** (2018) 075, [[arXiv:1712.07274](#)].
- [52] A. Brandhuber, M. Kostacinska, B. Penante, and G. Travaglini, *Higgs amplitudes from $\mathcal{N} = 4$ super Yang-Mills theory*, *Phys. Rev. Lett.* **119** (2017), no. 16 161601, [[arXiv:1707.09897](#)].
- [53] Q. Jin and G. Yang, *Analytic Two-Loop Higgs Amplitudes in Effective Field Theory and the Maximal Transcendentality Principle*, *Phys. Rev. Lett.* **121** (2018), no. 10 101603, [[arXiv:1804.04653](#)].
- [54] A. Brandhuber, M. Kostacinska, B. Penante, and G. Travaglini, *$Tr(F^3)$ supersymmetric form factors and maximal transcendentality Part I: $\mathcal{N} = 4$ super Yang-Mills*, *JHEP* **12** (2018) 076, [[arXiv:1804.05703](#)].

- [55] A. Brandhuber, M. Kostacinska, B. Penante, and G. Travaglini, *Tr(F^3) supersymmetric form factors and maximal transcendentality Part II: $0 < \mathcal{N} < 4$ super Yang-Mills*, *JHEP* **12** (2018) 077, [[arXiv:1804.05828](#)].
- [56] Q. Jin and G. Yang, *Hidden Analytic Relations for Two-Loop Higgs Amplitudes in QCD*, [[arXiv:1904.07260](#)].
- [57] K. Chetyrkin and F. Tkachov, *Integration by Parts: The Algorithm to Calculate beta Functions in 4 Loops*, *Nucl.Phys.* **B192** (1981) 159–204.
- [58] F. Tkachov, *A Theorem on Analytical Calculability of Four Loop Renormalization Group Functions*, *Phys.Lett.* **B100** (1981) 65–68.
- [59] R. H. Boels, Q. Jin, and H. Luo, *Efficient integrand reduction for particles with spin*, [[arXiv:1802.06761](#)].
- [60] D. A. Kosower and K. J. Larsen, *Maximal Unitarity at Two Loops*, *Phys. Rev.* **D85** (2012) 045017, [[arXiv:1108.1180](#)].
- [61] K. J. Larsen and Y. Zhang, *Integration-by-parts reductions from unitarity cuts and algebraic geometry*, *Phys. Rev.* **D93** (2016), no. 4 041701, [[arXiv:1511.01071](#)].
- [62] H. Ita, *Two-loop Integrand Decomposition into Master Integrals and Surface Terms*, *Phys. Rev.* **D94** (2016), no. 11 116015, [[arXiv:1510.05626](#)].
- [63] A. Georgoudis, K. J. Larsen, and Y. Zhang, *Azurite: An algebraic geometry based package for finding bases of loop integrals*, *Comput. Phys. Commun.* **221** (2017) 203–215, [[arXiv:1612.04252](#)].
- [64] S. Abreu, F. Febres Cordero, H. Ita, M. Jaquier, B. Page, and M. Zeng, *Two-Loop Four-Gluon Amplitudes from Numerical Unitarity*, *Phys. Rev. Lett.* **119** (2017), no. 14 142001, [[arXiv:1703.05273](#)].
- [65] S. Abreu, F. Febres Cordero, H. Ita, B. Page, and M. Zeng, *Planar Two-Loop Five-Gluon Amplitudes from Numerical Unitarity*, [[arXiv:1712.03946](#)].
- [66] W. Buchmuller and D. Wyler, *Effective Lagrangian Analysis of New Interactions and Flavor Conservation*, *Nucl. Phys.* **B268** (1986) 621–653.
- [67] J. A. Gracey, *Classification and one loop renormalization of dimension-six and dimension-eight operators in quantum gluodynamics*, *Nucl. Phys.* **B634** (2002) 192–208, [[hep-ph/0204266](#)]. [Erratum: *Nucl. Phys.*B696,295(2004)].
- [68] D. Neill, *Two-Loop Matching onto Dimension Eight Operators in the Higgs-Gluon Sector*, [[arXiv:0908.1573](#)].
- [69] R. V. Harlander and T. Neumann, *Probing the nature of the Higgs-gluon coupling*, *Phys. Rev.* **D88** (2013) 074015, [[arXiv:1308.2225](#)].
- [70] S. Dawson, I. M. Lewis, and M. Zeng, *Effective field theory for Higgs boson plus jet production*, *Phys. Rev.* **D90** (2014), no. 9 093007, [[arXiv:1409.6299](#)].
- [71] W. A. Bardeen, A. J. Buras, D. W. Duke, and T. Muta, *Deep Inelastic Scattering Beyond the Leading Order in Asymptotically Free Gauge Theories*, *Phys. Rev.* **D18** (1978) 3998.
- [72] S. Catani, *The Singular behavior of QCD amplitudes at two loop order*, *Phys. Lett.* **B427** (1998) 161–171, [[hep-ph/9802439](#)].

- [73] G. F. Sterman and M. E. Tejeda-Yeomans, *Multiloop amplitudes and resummation*, *Phys. Lett.* **B552** (2003) 48–56, [[hep-ph/0210130](#)].
- [74] Z. Bern, L. J. Dixon, and D. A. Kosower, *On-Shell Methods in Perturbative QCD*, *Annals Phys.* **322** (2007) 1587–1634, [[arXiv:0704.2798](#)].
- [75] Z.-G. Xiao, G. Yang, and C.-J. Zhu, *The rational parts of one-loop QCD amplitudes I: The general formalism*, *Nucl. Phys.* **B758** (2006) 1–34, [[hep-ph/0607015](#)].
- [76] G. Ossola, C. G. Papadopoulos, and R. Pittau, *On the Rational Terms of the one-loop amplitudes*, *JHEP* **05** (2008) 004, [[arXiv:0802.1876](#)].
- [77] T. Hahn, *Generating Feynman diagrams and amplitudes with FeynArts 3*, *Comput. Phys. Commun.* **140** (2001) 418–431, [[hep-ph/0012260](#)].
- [78] R. H. Boels and H. Luo, *A minimal approach to the scattering of physical massless bosons*, [arXiv:1710.10208](#).
- [79] A. V. Smirnov, *FIRE5: a C++ implementation of Feynman Integral REduction*, *Comput. Phys. Commun.* **189** (2015) 182–191, [[arXiv:1408.2372](#)].
- [80] R. N. Lee, *LiteRed 1.4: a powerful tool for reduction of multiloop integrals*, *J. Phys. Conf. Ser.* **523** (2014) 012059, [[arXiv:1310.1145](#)].
- [81] A. von Manteuffel and C. Studerus, *Reduze 2 - Distributed Feynman Integral Reduction*, [arXiv:1201.4330](#).
- [82] P. Maierhofer, J. Usovitsch, and P. Uwer, *Kira - A Feynman Integral Reduction Program*, [arXiv:1705.05610](#).
- [83] T. Gehrmann, E. Glover, T. Huber, N. Ikizlerli, and C. Studerus, *Calculation of the quark and gluon form factors to three loops in QCD*, *JHEP* **1006** (2010) 094, [[arXiv:1004.3653](#)].
- [84] T. Gehrmann and E. Remiddi, *Two loop master integrals for $\gamma^* \rightarrow 3$ jets: The Nonplanar topologies*, *Nucl. Phys.* **B601** (2001) 287–317, [[hep-ph/0101124](#)].
- [85] L. J. Dixon, E. W. N. Glover, and V. V. Khoze, *MHV rules for Higgs plus multi-gluon amplitudes*, *JHEP* **12** (2004) 015, [[hep-th/0411092](#)].
- [86] C. Duhr, *Hopf algebras, coproducts and symbols: an application to Higgs boson amplitudes*, *JHEP* **08** (2012) 043, [[arXiv:1203.0454](#)].
- [87] A. B. Goncharov, M. Spradlin, C. Vergu, and A. Volovich, *Classical Polylogarithms for Amplitudes and Wilson Loops*, *Phys. Rev. Lett.* **105** (2010) 151605, [[arXiv:1006.5703](#)].
- [88] Z. Bern, L. J. Dixon, and V. A. Smirnov, *Iteration of planar amplitudes in maximally supersymmetric Yang-Mills theory at three loops and beyond*, *Phys. Rev.* **D72** (2005) 085001, [[hep-th/0505205](#)].
- [89] P. Banerjee, P. K. Dhani, and V. Ravindran, *Two loop QCD corrections for the process Pseudo-scalar Higgs $\rightarrow 3$ partons*, *JHEP* **10** (2017) 067, [[arXiv:1708.02387](#)].
- [90] S. Badger, D. Chicherin, T. Gehrmann, G. Heinrich, J. M. Henn, T. Peraro, P. Wasser, Y. Zhang, and S. Zoia, *Analytic form of the full two-loop five-gluon all-plus helicity amplitude*, *Phys. Rev. Lett.* **123** (2019), no. 7 071601, [[arXiv:1905.03733](#)].

- [91] V. Del Duca, C. Duhr, R. Marzucca, and B. Verbeek, *The analytic structure and the transcendental weight of the BFKL ladder at NLL accuracy*, *JHEP* **10** (2017) 001, [[arXiv:1705.10163](#)].
- [92] T. Ahmed, P. Banerjee, A. Chakraborty, P. K. Dhani, and V. Ravindran, *The Curious Case of Leading Transcendentality: Three Point Form Factors*, [arXiv:1905.12770](#).
- [93] R. Bonciani, V. Del Duca, H. Frellesvig, J. M. Henn, M. Hidding, L. Maestri, F. Moriello, G. Salvatori, and V. A. Smirnov, *Evaluating two-loop non-planar master integrals for Higgs + jet production with full heavy-quark mass dependence*, [arXiv:1907.13156](#).